STRIATED MUSCLES OF THE BLACK BASSES (*MICROPTERUS*, CENTRARCHIDAE): MYOLOGICAL STASIS IN A GENERALIZED GROUP OF PERCOMORPH FISHES

W. Calvin Borden[1] and Miles M. Coburn[2]

ABSTRACT

Striated muscles of a generalized genus of percomorph fishes (*Micropterus*, Centrarchidae, Percomorpha) were described. Overall, myological variation was sparse among species of black bass. Variation took the form of minor variants in the size or shape of a muscle or of singular or incongruous variants characterized by abnormalities in a single specimen. The remaining myological variation occurred as mimicking variants and was shared irregularly among taxa. The lack of myological variation among black bass may well be correlated with the low degree of diversity exhibited in their ecology, life history, and external anatomy. However, the value of *Micropterus* in systematic and evolutionary studies is not compromised by morphological stasis. Instead, because *Micropterus* and other conserved lineages have been minimally responsive to ecological factors, they are valuable as outgroups to polarize character states, as identifiers of vicariant events leading to allopatric speciation, and as exemplars for studying the evolutionary mechanism of stabilizing selection. In addition, the description and assessment of myological variation in this generalized percomorph will be useful in future studies of comparative anatomy, functional morphology, and higher level systematics.

Key Words: Black bass, Centrarchidae, *Micropterus*, Myology, Stasis.

TABLE OF CONTENTS

Introduction 110
Methods 110
Material Examined 112
Results and Myological Descriptions 112
- Muscles of the Cheek 112
- Muscles of the Ventral Surface of the Head 116
- Muscles Serving the Dorsal Elements of the Branchial Arches 117
- Muscles Serving the Ventral Elements of the Branchial Arches 118
- Muscles Between the Pectoral Girdle and the Skull, Hyoid, and Branchial Arches 120
- Muscles of the Pectoral Fin 121
- Muscles of the Pelvic Fin 122
- Muscles of the Caudal Fin 126
- Notes on Other Features of the Soft Anatomy in *Micropterus* species 128

Discussion 129
- Myological Notes 129
- Myological Variation 129
- Macroevolutionary Patterns 130
- Phylogenetic Utility 131

Acknowledgements 132
Literature Cited 132

[1]Department of Biological, Geological, and Environmental Sciences, Cleveland State University, Cleveland, OH 44115; <w.c.borden@csuohio.edu>
[2]Department of Biology, John Carroll University, University Heights, OH 44118; <coburn@jcu.edu>

Borden, W.C. and M.M. Coburn. 2008. Striated muscles of the black basses (*Micropterus*, Centrarchidae): Myological stasis in a generalized group of percomorph fishes. Florida Museum. Nat. Hist. Bull. 47(4):109-136. [End of volume]

INTRODUCTION

The myology of fishes is an under-described morphological system relative to osteology. This is unfortunate because it has been shown to be relevant in determining phylogenetic relationships across a variety of diverse fish groups and taxonomic levels (e.g. tetradontiforms - Winterbottom 1974b; acanthurids – Winterbottom 1993; teleosts - Greenwood & Lauder 1981; cottoids - Yabe 1985; cirrhitoids – Greenwood 1995; acanthomorphs - Mooi & Gill 1995; nasines - Borden 1999; siluriform families - Diogo 2005; notothenioids - Iwami 2004; actinopterygians - Springer & Johnson 2004; basal acanthomorphs - Wu & Shen 2004; bony fish and tetrapods – Diogo & Abdala 2007). We initiated the current study to (1) describe a relatively unknown character system, striated muscles, in a generalized percomorph genus, (2) evaluate the utility of myology in resolving species level relationships among the black bass (*Micropterus*, Centrarchidae), and (3) contribute to the development of a myological data base suitable for higher level systematic studies among percomorphs.

The phylogenetic affinities of Centrarchidae within Percomorpha are unknown although centrarchids are considered basal members of the order. The family is monophyletic and consists of eight genera with 31 species inhabiting freshwaters, mostly in eastern North America, and known commonly as black bass, sunfish, rock bass, and crappies (Nelson 2006). The genus *Micropterus* Lacépède (1802) is monophyletic and is comprised of seven species, the redeye bass (*M. coosae*), the shoal bass (*M. cataractae*), the Suwannee bass (*M. notius*), the Guadalupe (*M. treculii*), and three species which have recognizable subspecies: the smallmouth bass (*M. dolomieu*: *dolomieu* and *velox*), the spotted bass (*M. punctulatus*: *henshalli* and *punctulatus*), and the largemouth bass (*M. salmoides*: *floridanus* and *salmoides*). Black bass have been identified as the basal clade of centrarchids (Ramsey 1975; Wainwright & Lauder 1992; Mabee 1993) or a derived clade either as the sister group to *Lepomis* (Branson & Moore 1962; Avise et al. 1977; Near et al. 2005), or with unresolved affinities (Roe et al. 2002).

The interspecific relationships of *Micropterus* species have also varied considerably. Bailey (1938) and Hubbs and Bailey (1940) envisioned two lineages of black bass, one consisting solely of *M. salmoides* placed in the genus *Huro* (Fig. 1A). Branson and Moore (1962) recognized six species and identified *M. salmoides* as the basal lineage based on a detailed analysis of the acustico-lateralis system (Fig. 1B). Ramsey (1975) grouped seven species into three lineages with *M. salmoides* comprising one lineage, and *M. coosae* and *M. dolomieu* comprising a second lineage (Fig. 1C). These morphological hypotheses were followed by a series of molecular analyses using phylogenetic methods (Fig 1D, Johnson et al. 2001; Fig. 1E, Kassler et al. 2002; Fig. 1F, Near et al. 2003, 2005). While the results of the Johnson et al. (2001) study resembled those morphological hypotheses with *M. salmoides* as the basal clade, the remaining molecular studies suggested new phylogenetic relationships. Kassler et al. (2002), employing meristic and molecular characters, recovered *M. salmoide*s deeply nested in the tree and a non-sister group relationship between *M. punctulatus henshalli* and *M. punctulatus punctulatus* (Fig. 1E). Most recently, Near et al. (2003, 2005) recovered a fully resolved tree supporting a *M. dolomieu-M. punctulatus* clade as the sister group to the remaining black bass (Fig. 1F).

Black bass are high trophic level predators primarily of fishes and crayfishes (Scott & Crossman 1973; Koppelman & Garrett 2002) and well known as sport fishes. As a consequence, numerous studies have investigated facets of their ecology, reproduction, life history, and behavior (see Philipp & Ridgway 2002 as a starting point). In addition, various anatomical components have been described as exemplars in the context of functional morphology (Wainwright & Lauder 1992; Higham 2007), kinematics (Lauder 1982), ecomorphology (Norton & Brainerd 1993; Wintzer & Motta 2005), descriptive osteology (Shufeldt 1900; Blair & Brown 1961; Mabee 1988), ontogeny (Mabee 1993), and pigment patterns (Mabee 1995). A complete morphological appraisal of a relatively conservative anatomical system (i.e. myology) promotes a fuller understanding of the comparative anatomy, functional morphology, and systematics of these fishes.

METHODS

Sample size can adversely affect phylogenetic results particularly if character state variation within the taxonomic unit is not identified. A protocol for detecting myological variants was put forth by Raikow et al. (1990) and subsequently modified by Kesner (1994). Their models suggested that at least 10 specimens of a reference species should be bilaterally dissected in a search for variable character states. Variants were categorized as "incongruous" (abnormal and nonfunctional variation due to a malformation), "mimicking" (an atypical condition in one species that is typical for a different species), "minor" (slight variation in size, shape, position and perhaps resulting from nonbiological causes), and "singular" (atypical but not nonfunctional, and not present in other taxa) (Raikow et al. 1990). Incongruous, minor,

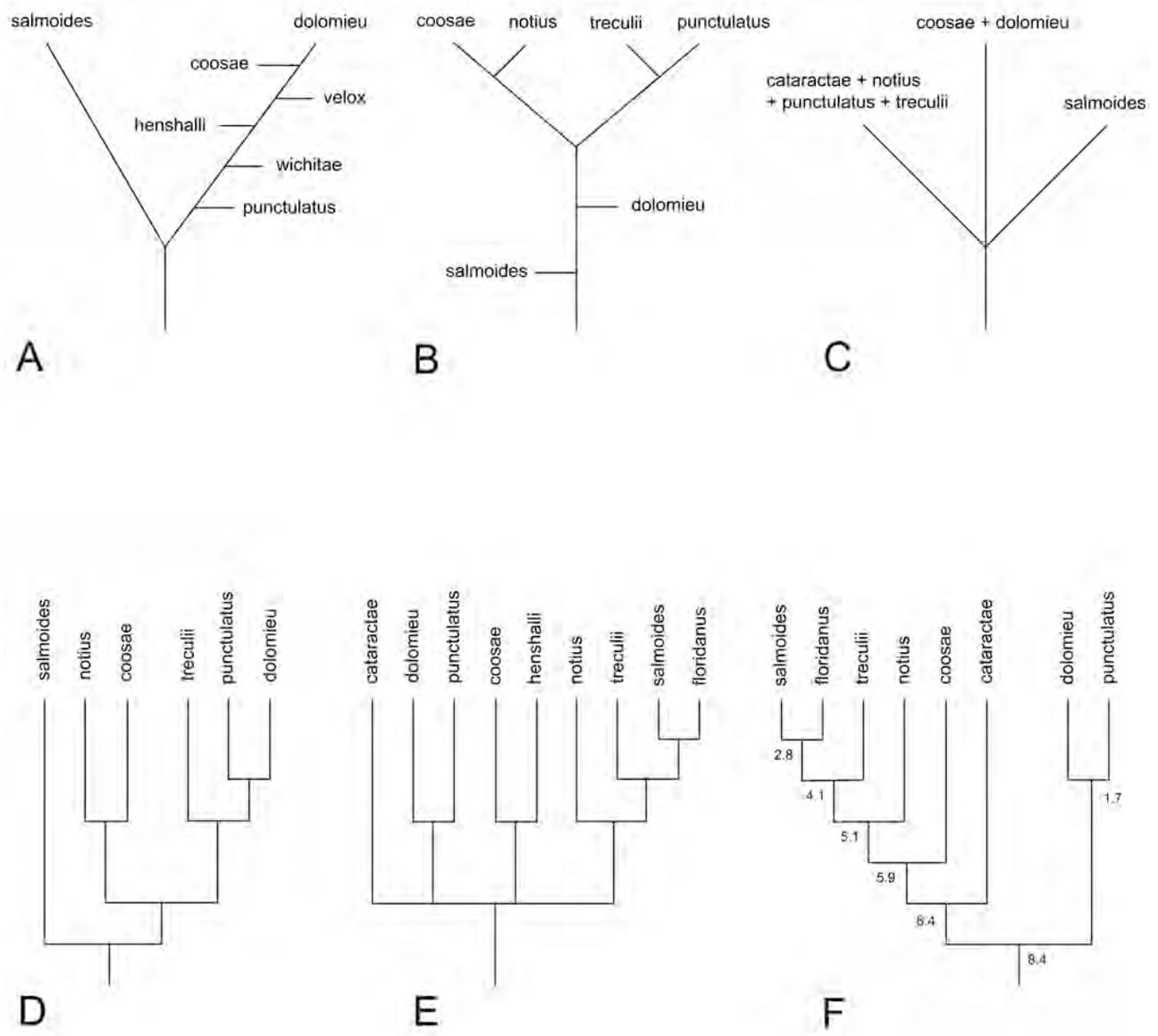

Figure 1. Proposed phylogenetic relationships among the black bass. Each hypothesis is based on a different data set and tree building criterion, if any. A. Hubbs and Bailey (1940, Fig. 1). "dolomieu" and "velox" are subspecies of *M. dolomieu*. "henshalli", "punctulatus", and "wichitae" are subspecies of *M. punctulatus*. B. Branson and Moore (1962, Fig. 15). C. Ramsey (1975) included 2 subspecies in *M. salmoides* and *M. dolomieu* each and 3 subspecies in *M. punctulatus*. D. Johnson et al. (2001, Fig. 2). E. Kassler et al. (2002, Fig. 6). F. Near et al. (2005, Fig. 7). Near et al (2003) switched the position of "cataractae" and "coosae". The numbers located at each node are age estimates in "millions of years ago" using a fossil cross-validation methodology (Near et al. 2005).

and singular variants are phylogenetically uninformative; mimicking variants create homoplasies in the form of convergences or parallelisms. Raikow et al. (1990) recommended initial dissections of a reference species to identify and eliminate minor and incongruous variants. Single bilateral dissection and at least two unilateral dissections should be undertaken in the remaining species to resolve mimicking and singular variants. Alternatively, in the absence of 10 specimens for a given species, four to five specimens of several species should be dissected (Kesner 1994).

Lacking a series of 10 specimens, *M. coosae*, *M. d. dolomieu*, and *M. s. salmoides* were dissected for seven, five, and eight specimens respectively of which

four, four, and six specimens were bilaterally dissected. In all specimens examined, muscles of the branchial and hyoid arches, pectoral, pelvic, and caudal fins were bilaterally dissected. Muscles of head, cheek, jaws, suspensorium, and those connecting any two components of the head, suspensorium, and fins were dissected bilaterally in at least one specimen. Specimens were dissected sequentially and in random order excepting most specimens of *M. d. dolomieu* and *M. s. salmoides*, which were dissected at the beginning of the study to assess the prevalence of the four variant classes.

Striated muscle terminology follows Winterbottom (1974a); nerves follow Freihofer (1963). Muscle descriptions represent a consensus or generalized form of each species, thus averaging out the effects of minor variation such as muscle proportions or muscle origins on bones with fimbricate sutures (e.g. prootic and pterotic suture). Swimbladder and subcutaneous muscles were not observed, median fin and eye muscles were not examined, and body and carinal muscles were not described in detail except as relevant to muscles described below. Roman numerals were used to denote muscles; Arabic numbers were used to denote bones. Singular and incongruous variants were noted under the appropriate muscle and checked against antimeres and other specimens. Intraspecific and mimicking variation is listed in Table 1. Soft anatomical features such as the number and structure of pyloric caecae and the nasal rosette were also described. Morphological conditions in outgroup species were described for characters variable only among *Micropterus* species or for incongruous and singular variants.

Fish were fixed in 10% formalin and stored in 70-75% ethyl alcohol. Specimens were dissected using a Nikon SMZ-U microscope and drawn using a camera lucida attachment on a Leica MZ125 microscope. Small and questionable muscle fibers were stained with a modified iodine solution (Bock & Shear 1972) to highlight them against non-muscle tissue. Following dissection, some specimens were cleared and double stained for bone (alizarin red-S) and cartilage (Alcian blue) using modified protocols of Potthoff (1984) and Taylor and Van Dyke (1985).

Scientific names follow Nelson et al. (2004) with the following additions that recognized subspecific status in *M. dolomieu* [*dolomieu* and *velox*], *M. punctulatus* [*henshalli* and *punctulatus*] (following Hubbs & Bailey 1940), and *M. salmoides* [*floridanus* and *salmoides*] (following Bailey & Hubbs 1949). Although Kassler et al. (2002) argued for the promotion of *M. s. floridanus* and *M. s. salmoides* to specific status based on meristic and molecular data, we retain them as subspecies following the recommendation of Nelson et al. (2004) for additional analysis.

MATERIAL EXAMINED

Institutional abbreviations follow Leviton et al. (1985). The number of specimens dissected and their standard length(s) in millimeters follows the catalog number.

Micropterus. — (1): *M. cataractae* Williams & Burgess 1999, ROM 82445, 1 (216.2 mm SL); UMMZ 168752, 1 (102.8 mm SL). (2): *M. coosae* Hubbs & Bailey 1940, OSUM 105229, 1 (104.3 mm SL); ROM 82449, 1 (116.0 mm SL); ROM 82450, 1 (126.1 mm SL); UF 86268, 1 (131.8 mm SL); UF 86313, 1 (122.2 mm SL); UF 89989, 1 (154.7 mm SL); USNM 168075, 1 (98.7 mm SL). (3): *M. d. dolomieu* Lacépède 1802, CAS 13020 C&S, 1 (77.2 mm SL); OSUM 102599, 1 (173.2 mm SL); OSUM 102600, 1 (155.2 mm SL); ROM 1783CS, 1 (178.3 mm SL); ROM 82436, 1 (248.8 mm SL); ROM 82437, 1 (133.2 mm SL). (4): *M. d. velox* Hubbs & Bailey 1940, UMMZ 116802, 1 (121.6 mm SL); UMMZ 128680, 1 (120.7 mm SL). (5): *M. notius* Bailey & Hubbs 1949, UF 57323, 1 (187.6 mm SL); UF 58761, 2 (131.8 – 145.2 mm SL, fish labeled "4" and "5" respectively by UF); TU 9775, 2 (107.4 – 152.3 mm SL). (6): *M. p. henshalli* Hubbs & Bailey 1940, UAIC 10587.15, 1 (154.3 mm SL); UAIC 12652.19, 1 (132.8 mm SL). (7): *M. p. punctulatus* (Rafinesque 1819), OSUM 102597, 1 (153.4 mm SL); OSUM 102598, 1 (144.7 mm SL); USNM 251991, 2 (88.0 - 95.4 mm SL). (8): *M. s. floridanus* (Lesueur 1822), UMMZ 158634, 1 (128.8 mm SL); UMMZ 163350, 1 (125.6 mm SL). (9): *M. s. salmoides* (Lacépède 1802), CAS 19030 C&S, 1 (60.6 mm SL); ROM 1780CS, 1 (170. mm SL); ROM 1781CS, 1 (159.1 mm SL); ROM 1782CS, 1 (138.2 mm SL); ROM 82435, 1 (176.5 mm SL); ROM 82446, 4 (153.2 – 219.4 mm SL). (10): *M. treculii* (Vaillant & Bocourt 1874), OSUM 105227, 1 (254.0 mm SL); ROM 1784CS, 1 (253.0 mm SL); UMMZ 136849, 1 (112.8 mm SL); UMMZ 220247, 1 (137.2 mm SL).

Centrarchids. — (1): *Ambloplites ariommus* Viosca 1936, ROM 82444, 1 (105.2 mm SL). (2): *Centrarchus macropterus* (Lacépède 1801), UMMZ 164961, 1 (124.8 mm SL). (3): *Lepomis cyanellus* Rafinesque 1819, ROM 82438, 1 (81.1 mm SL). (4): *Lepomis gibbosus* (Linnaeus 1758), ROM 82439, 1 (113.6 mm SL). (5): *Pomoxis nigromaculatus* (Lesueur 1829), ROM 82440, 1 (152.3 mm SL).

RESULTS AND MYOLOGICAL DESCRIPTIONS

I. MUSCLES OF THE CHEEK

The ligamentum primordium attaches tendinously

on the dorsolateral surface of the maxilla and arcs posteriorly and ventrally to attach on the lateral surface of the angular (angulo-articular) anterior of the quadrate-angular articulation.

Adductor mandibulae (A1, A2, A3, Aù , Figs. 2-5, 8). All sections of the adductor mandibulae are graded to varying degrees, and the extensive grading complicates assignment of fibers to a specific section. After removal of the skin and infraorbitals, the adductor mandibulae occupies the lateral side of the suspensorium in the space bounded by the orbit, preopercle, and jaws. The lateralmost section of the adductor mandibulae is A1. Section A1 is described as two bundles of unequal size. The dorsalmost of the two sections originates on the preopercle, anterodorsal face of the hyomandibula, and base of the levator arcus palatini. The ventral border is separable from the ventral and main mass of A1 only laterally as fibers are graded medially. As the dorsal section passes anteriorly, it rolls medially over the main mass of A1 and grades into a medial aponeurosis shared by several sections of the adductor mandibulae. Fibers of the main bundle of A1 originate primarily on the preopercle but also include the hyomandibula. Insertion includes the ligamentum primordium particularly at the anterodorsal corner of the muscle and the aforementioned medial aponeurosis. In addition, a well-developed tendon arises from the anteromedial corner of the muscle mass, runs parallel to the ligamentum primordium, and inserts on the medial surface of the maxilla at the level of the ligamentum primordium. Insertion on the medial surface of the maxilla suggests that it is A1â; however, the lack of a distinct origin from the palatal arch or suspensorium and its dorsolateral position relative to A2 preclude its identification as A1â.

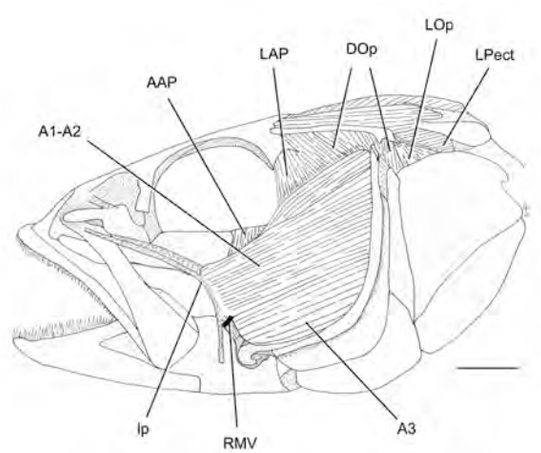

Figure 2. Left, lateral view of the superficial cheek musclulature of *M. p. henshalli* (UAIC 12652.19, 132.8 mm SL). Anterior is to the left. Scale bar = 5 mm. Abbreviations: A1, A2, A3 – sections of the adductor mandibulae; AAP – adductor arcus palatine; DOp – dilatator operculi; LAP – levator arcus palatini; LOp – levator operculi; lp – ligamentum primordium; LPect – levator pectoralis; RMV – ramus mandibularis V.

A2 originates on the preopercle and hyomandibula and is inseparable from A1 due to extensive grading. Minor grooves and lateral separations were occasionally present in the fused A1- A2á bundle, but disappeared medially due to extensive grading and, therefore, were not given subsection status. Anterior and more dorsal fibers of A2 grade into the medial aponeurosis shared by the bundles of A1 while more ventral fibers grade into A*ù* via a myocommatum. A tendon arises from the anteroventral corner of the A1- A2 muscle mass and inserts on the medial side of the angular in the Meckelian fossa ventral to the cartilage.

Ramus mandibularis V of the 5th cranial nerve (trigeminal nerve) is medial to A1- A2 and lateral to a single section of muscle identified as A3. A3 originates on the quadrate, symplectic, hyomandibula, preopercle, metapterygoid, and base of the levator arcus palatini at the metapterygoid. The posterior border of A3 is notched weakly giving it a chevron shape. Dorsal fibers of A3 attach to the tendon of A1-A2, the shared medial aponeurosis, and A*ù* . More ventral fibers of A3, originating on the quadrate and symplectic, run near horizontal and give rise to a tendon that inserts on the medial side of the angular in the Meckelian fossa dorsal to the cartilage and near its posterior end. This tendon is lateral to the tendon from A1-A2.

A*ù* attaches on the medial side of the lower jaw from the intermandibularis at its anterior end and extends posteriorly via a strong tendon to originate on the quadrate, preopercle, and symplectic. The tendon of A*ù* is medial to the tendons from sections A1-A2 and A3; however, fibers of A*ù* are heavily graded with both tendons and determining which fiber belongs to which section is both frustrating and fruitless as this pattern is consistent among *Micropterus* species.

Levator arcus palatini (LAP, Figs. 2, 3, 7). This muscle is a large bundle forming the posterior wall of the orbit. It originates on the sphenotic and fans out onto the metapterygoid and hyomandibula with a few fibers extending to the adductor arcus palatini. The origin does not appear to include the frontal dorsally or prootic medially. The posterior border passes medial to the anterior border of the dilatator operculi, but the two muscles have only a few, if any, graded fibers.

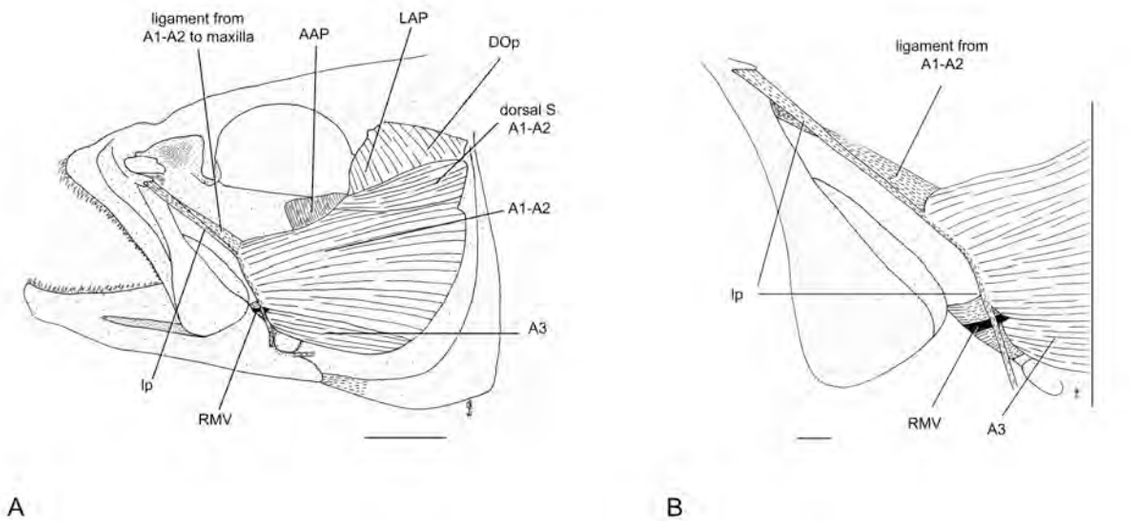

Figure 3. Left, lateral view of the superficial cheek musculature of *M. cataractae* (UMMZ 168752, 102.8 mm SL). Anterior is to the left. A. as above. Scale bar = 5 mm. B. Detailed view of the tendons inserting on the medial side of the maxilla and fibers passing to the medial side of the lower jaw. Scale bar = 1 mm. Abbreviations as in Figure 2.

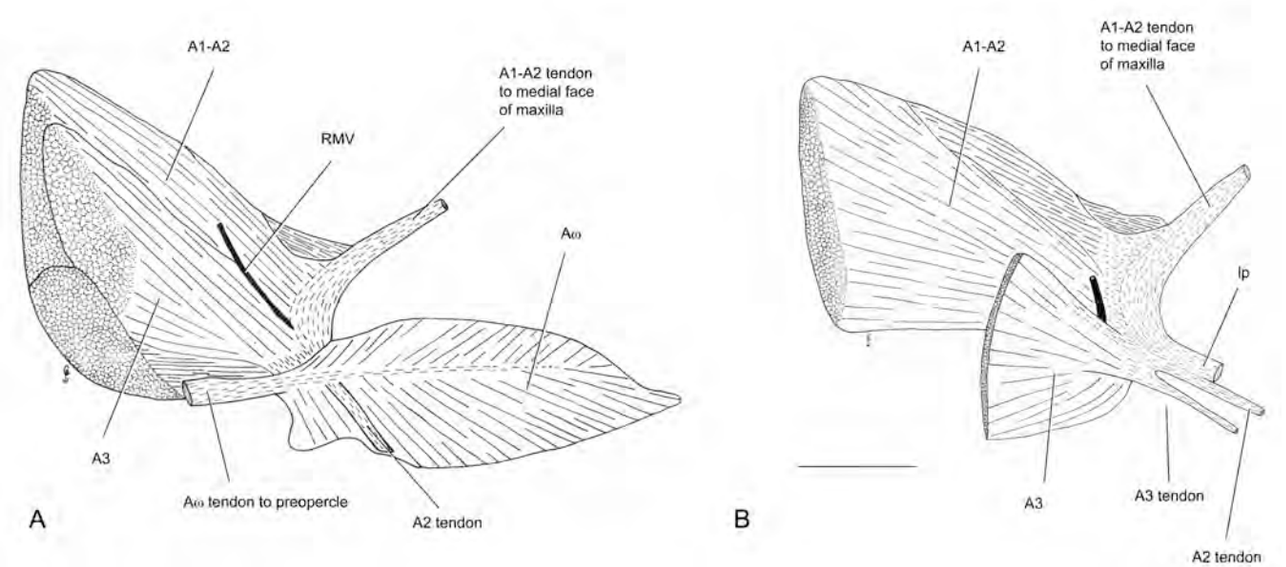

Figure 4. Medial view of the cheek musculature of *M. p. henshalli* (UAIC 12652.19, 132.8 mm SL). Anterior is to the right. Scale bar = 5 mm. A. The lower jaw has been removed, and the tendon of Aù to the suspensorium and preopercle has been cut. B. As above with Aù removed and most of A3 cut and removed. Abbreviations: Aù – medial section of the adductor mandibulae; as in Figure 2.

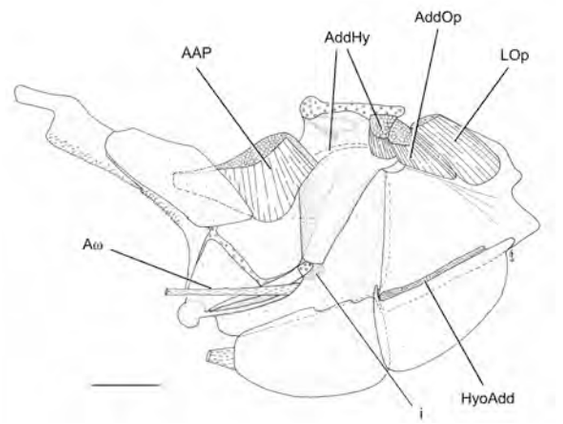

Figure 5. Medial view of the muscles connecting the cranium to the right suspensorium and opercular series of *M. s. floridanus* (UMMZ 163350, 125.6 mm SL). Anterior is to the left. Scale bar = 5 mm. Abbreviations: AddHy – adductor hyomandibulae; AddOp – adductor operculi; HyoAdd – hyohyoides adductores; i – site of interhyal articulation; as in Figures 2 and 4.

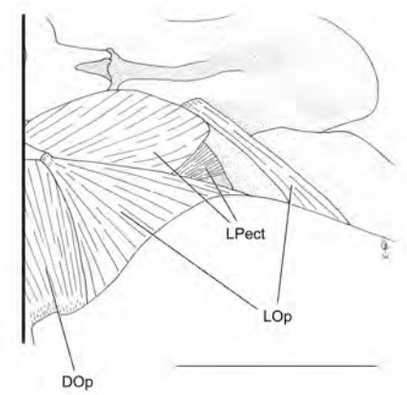

Figure 6. Left, lateral view of the posterior muscles connecting the cranium and opercular series of *M. p. punctulatus* (OSUM 102598, 144.7 mm SL). Anterior is to the left. Scale bar = 5 mm. Abbreviations as in Figure 2.

Dilatator operculi (DOp, Figs. 2, 3, 6, 7). This muscle has the shape of an inverted triangle with a broad origin on the sphenotic, pterotic, and hyomandibula. It tapers ventrally and inserts on the dilatator process of the opercle. Fibers pass medial to the dorsal tip of the preopercle. The posterior border is medial to the levator operculi; fibers of the two muscles are not graded.

Levator operculi (LOp, Figs. 2, 5-7). The origin is confined to the pterotic but the muscle quickly fans out onto the medial, dorsal surface of the opercle. A small, autonomous section of fibers originates from the posttemporal and inserts on the medial, dorsal surface of the opercle posterior to the main mass. This posterior section is weakly developed and lies within connective tissue running from the skull to the opercle. This posterior section was the most diffuse and smallest in both specimens of *M. cataractae*, and absent in *Lepomis cyanellus* (ROM 82438).

Adductor arcus palatini (AAP, Figs. 2, 3, 5). This muscle forms the posterior half of the orbit floor. It originates on the prootic and parasphenoid and inserts on the metapterygoid and mesopterygoid. Posteriorly it is continuous and graded heavily with the adductor hyomandibulae.

Adductor hyomandibulae (AddHy, Figs. 5, 7). This muscle is continuous with the posterior border of the adductor arcus palatini. It inserts solely on the medial side of the hyomandibula. The origin includes the prootic, pterotic, and anteriodorsal corner of the intercalar.

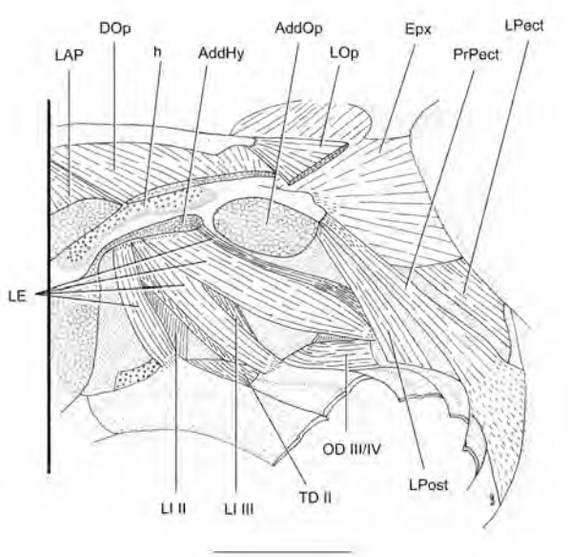

Figure 7. Left, lateral view of muscles connecting the cranium to the suspensorium and pectoral girdle and the dorsal muscles of the branchial gill arches of *M. p. punctulatus* (OSUM 102598, 144.7 mm SL). Anterior is to the left. Scale bar = 5 mm. Abbreviations: Epx – epaxialis; h – site of hyomandibular articulation; LE – levator externus; LI – levator internus; LPost – levator posterior; OD – obliquus dorsalis; PrPect – protractor pectoralis; TD – transverses dorsalis; as in Figures 2 and 5.

The origin is linear on the neurocranium (sphenotic-pterotic) along the medial side of the hyomandibula's articulation with the skull. The muscle is bulkier on either side of this articulation.

Adductor operculi (AddOp, Figs. 5, 7). The adductor operculi originates on the intercalar and extends ventrally to the suture with the exoccipital but not onto the exoccipital. The origin lies posterior to the adductor hyomandibulae and anterior to the levator posterior. The adductor operculi is separable from the latter but may grade with the adductor hyomandibulae. Insertion is on the medial side of the opercle dorsal to a horizontal bony ridge, and posterior to the opercle-hyomandibula articulation and levator operculi.

II. MUSCLES OF THE VENTRAL SURFACE OF THE HEAD

Intermandibularis (IntM, Fig. 8). The intermandibularis originates on the medial surface of the dentary, on either side of the symphysis, and meets its antimere at the ventral midline in the absence of a raphé. The muscle is a flattened sheet lying in a frontal plane.

Protractor hyoidei (PrHy, Fig. 8). The anterior border of this muscle is bifurcated to accommodate its origin on the medial surface of the dentary above and below the intermandibularis. Anteriorly the antimeres are held together along the ventral midline via a septum but diverge posteriorly. Two myocommata are present posteriorly. Insertion is on the lateral side of the anterior ceratohyal with the posteroventral fibers passing laterally to branchiostegal rays 1 and 2, but medially to ray 3. An exception to this pattern was *M. coosae* (UF 86313), in which the right antimere passes lateral to branchiostegal rays 1-3 and medial to ray 4; however, the left antimere follows the "normal" pattern. It may be more accurate to note that the protractor hyoidei passes medial to the first branchiostegal ray having a well-developed head (usually the third ray) that also articulates on the lateral side of the anterior ceratohyal. Branchiostegal rays anterior to this ray lack such well-developed heads and abut the ventral edge of the anterior ceratohyal, not its lateral surface.

Hyohyoides inferioris. This muscle running from the urohyal to the hyoid arch is absent.

Hyohyoidei adductores (HyoAdd, Fig. 9). The adductor bundles originate primarily on the medial side of the opercle and insert on the dorsoposterior surfaces of the posteriormost branchiostegal rays. Additional bundles are isolated distally between branchiostegal rays. In general, adductor fibers parallel the ventral borders of the anterior and posterior ceratohyals.

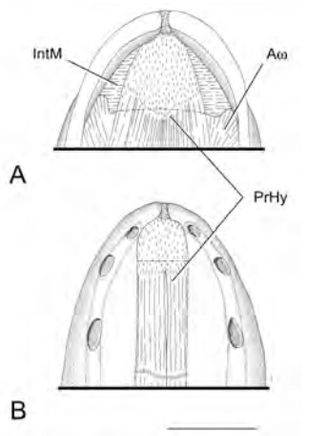

Figure 8. A. Dorsal and B. ventral view of the lower jaws and of *M. coosae* (ROM 82449, 116.0 mm SL). Anterior is to the left. Unfilled area of A is toothed. Scale bar = 5 mm. Abbreviations: IntM – intermandibularis; PrHy – protractor hyoidei; as in Figure 4.

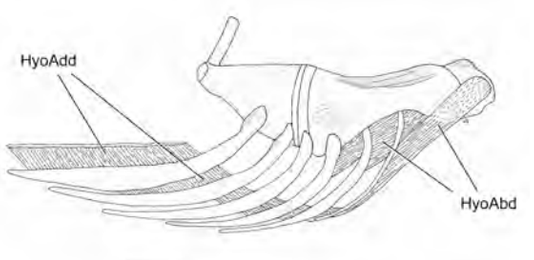

Figure 9. Right, lateral view of the hyoid arch minus the urohyal of *M. d. dolomieu* (OSUM 102600, 155.2 mm SL). Anterior is to the right. Scale bar = 5mm. The branchiostegals have been spread and not all fibers of the hyohyoidei abductores were drawn including the antimere originating from the hypohyals. Abbreviations: HyoAbd – hyohyoideus abductores; as in Figure 5.

Hyohyoidei abductores (HyoAbd, Fig. 9). The abductors are composed of many isolated bundles. The largest bundle originates tendinously on the dorsal and ventral hypohyals. This bundle crosses the midventral line and attaches to the medial surfaces of branchiostegal rays 1 and 2. Antimeres overlap at the origin with the left antimere (left side of hypohyals to right branchiostegal rays) ventral to the right antimere. Additional bundles originate muscularly on the ventral side of the anterior ceratohyal and insert on the medial, proximal surfaces of adjacent branchiostegal rays. In general, abductor bundles are orientated obliquely relative to the ventral borders of the anterior and posterior ceratohyals.

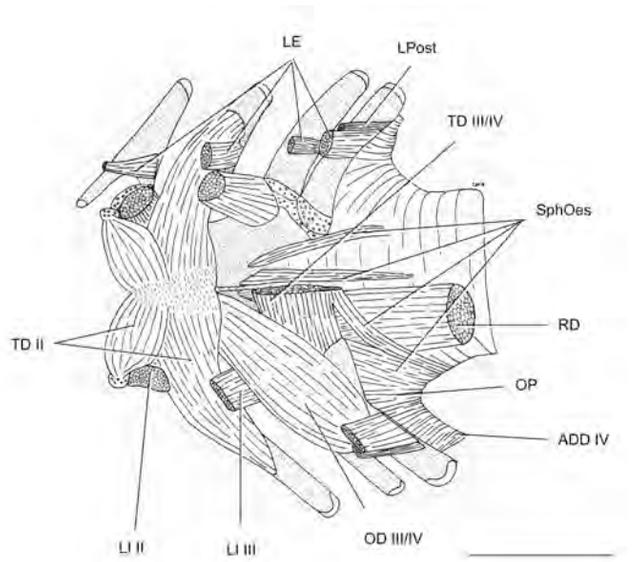

Figure 10. Dorsal view of the branchial gill arch muscles of *M. p. henshalli* (UAIC 12652.19, 132.8 mm SL). Anterior is to the left. Scale bar = 5 mm. The left epibranchial 1 has been removed as has the right pharyngobranchial 1. The right antimere of the retractor dorsalis, obliquus dorsalis III/IV, and transversus dorsalis IV have been removed. Abbreviations: Add – adductor; OP – obliquus posterior; RD – retractor dorsalis; SphOes – sphincter oesophagi; as in Figure 7.

III. MUSCLES SERVING THE DORSAL ELEMENTS OF THE BRANCHIAL ARCHES

Levatores externi (LE I-IV, Figs. 7, 10, 11). Four muscles, each a levator externus, constitute the levatores externi with each bundle serving the dorsal elements of one of the first four gill arches. Levatores externi I and II originate primarily on the prootic while III and IV originate primarily on the pterotic although all four muscles probably share both the prootic and pterotic. Levator externus I is nearly vertical but the remaining externi muscles are orientated obliquely. Levatores externi III and IV are closely appressed but not graded. Levator externus I inserts on epibranchial 1 anterolateral to its articulation with the interarcual cartilage. Levator externus II inserts on a raised dorsoposterior ridge of epibranchial 2; levator externus III inserts on a well developed uncinate process of epibranchial 3, and levator externus IV inserts on a raised ridge of epibranchial 4 that is lateral to the uncinate process but medial to a very small levator process. Insertion sites move distally from levator externus I to IV.

Levatores interni (LI II-III, Figs. 7, 10). Two muscles, each a levator internus, serve the dorsal elements of either the second or third gill arch. They originate on the prootic and pterotic medial to the levatores externi. Levator internus II is medial to III, and they form an "X" in lateral view. Levator internus II inserts on the dorsal surface of pharyngobranchial 2 adjacent to its articulation with the interarcual cartilage. Levator internus II inserts on the dorsal surface of pharyngobranchial 3 adjacent to its articulation with epibranchial 3. In *M. treculii* (UMMZ 136849), fibers of levator internus III also insert on the cartilaginous end of epibranchial 3 at its articulation with pharyngobranchial 3.

Levator posterior (LPost, Figs. 7, 10). The levator posterior is well developed and separated from the externi and interni muscles. It originates on the intercalar, posterior of the adductor operculi, at the base of the 'stump' that articulates with the posttemporal. It inserts

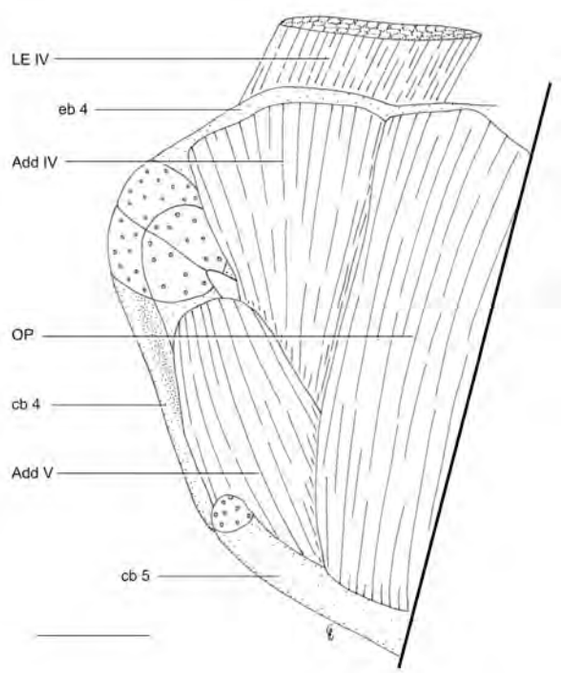

Figure 11. Posterior view of the left fourth and fifth branchial gill arches and muscles of *M. d. velox* (UMMZ 128680, 120.7 mm SL). The esophagus is to the right. Scale bar = 1 mm. The sphincter oesophagi grades into the obliquus posterior medially. The protractor pectoralis has been removed. Muscle fibers extend ventrally to the level of the epibranchial-ceratobranchial articulation before grading into the branchial wall. The latter is attached to the posterior surfaces of epibranchial 4 and ceratobranchials 4 and 5. Abbreviations: cb 4 – ceratobranchial 4; cb 5 – ceratobranchial 5; eb 4 – epibranchial 4; as in Figures 7 and 10.

on the dorsal, distal surface of epibranchial 4 anterior to levator externus IV.

Obliquus dorsalis (OD III/IV, Figs. 7, 10). A single bundle originates from the dorsal surfaces of epibranchials 3 and 4 and extends medially to insert on the dorsal surface of pharyngobranchial 3. Fibers along the epibranchials are heavily graded.

Transversi dorsales (TD II, III/IV, Figs. 7, 10). Transversus dorsalis II consists of two graded bundles. An anterior circular bundle arises from the dorsolateral surface of pharyngobranchial 2 and passes medially where it attaches to its antimere via a raphé. A more posterior bundle arises along the dorsal surface of epibranchial 2 and passes to the dorsal midline where it attaches to its antimere via a raphé. The posterior border of the circular section is dorsal to the more posterior section but the two sections are heavily graded. Ventrally the bundles adhere to the dorsal side of the skin lining the buccal cavity along the dorsal midline. Dorsally, the muscle abuts the parasphenoid. Springer and Johnson (2004) noted a small accessory cartilage on the anterodorsal tip of pb2 as part of the origin of TD II in cleared and stained material of *M. dolomieu*. In essence, this cartilage lies on the "free" and cartilaginous end of pb2 adjacent to the interarcual cartilage. Such a cartilage was not observed during the dissection of the dorsal gill arches prior to double-staining. Eight specimens were cleared and stained (one each of *M. coosae*, *M. d. dolomieu*, *M. notius*, *M. p. punctulatus*, *M. treculii*, and three *M. s. salmoides*) following dissection. The first author noticed what he would call a cartilaginous bud on one specimen of *M. d. dolomieu* and *M. s. salmoides*. However, confidence in this interpretation is not high since the TD II and/or pb's were removed in many dissections and consequently could have removed any autogenous or bud-like cartilages.

A transversus dorsalis III/IV bundle originates on the dorsal surfaces of epibranchial 3 and pharyngobranchial 3 and often includes the medial cartilaginous end of epibranchial 4 and dorsal surface of pharyngobranchial 4. Fibers extend medially to join its antimere in the absence of a raphé. The posterior border of the bundle is usually separable from fibers of the sphincter oesophagi.

Obliquus posterior (OP, Figs. 10-11). This is a well-developed muscle posterior to both of the adductor muscles. It is attached to the posterior side of ceratobranchial 5 and runs dorsally to insert on the posterior surface of epibranchial 4, medial to levator externus IV. The obliquus posterior grades into the sphincter oesophagi medially.

Adductores (Add IV-V, Figs. 10, 11). Adductor IV connects ceratobranchial 4 and epibranchial 4. The insertion on epibranchial 4 is lateral to the obliquus posterior. Adductor V connects ceratobranchials 4 and 5; however, fibers may extend onto the cartilaginous end of epibranchial 4 at its articulation with ceratobranchial 4. Adductor V is posterior to adductor IV.

Retractor dorsalis (RD, Fig. 10). The retractor dorsalis is a large muscle originating on the ventral surfaces of vertebral centra 2 and 3, with some fibers on the posterior half of vertebral centrum 1. The left and right muscles pass anteroventrally to insert on the dorsal surfaces of pharyngobranchials 3 and 4.

Interbranchiales abductors. The abductors connect the proximal, lateral bases of the filaments to the bony arches.

Interbranchiales adductores (IntBAdd, Fig. 12). These bundles originate on the base of the gill filament of one hemibranch and attach distally to the gill filament of the opposite hemibranch. Thus, this is a Type I adductor as defined by Pasztor and Kleerekoper (1962).

IV. MUSCLES SERVING THE VENTRAL ELEMENTS OF THE BRANCHIAL ARCHES

The ventral side of the branchial arches is characterized by a distinct pattern of ligaments connecting the bony elements. From the ventral surface of basibranchial 3 a cupula (cartilaginous pedicle) arises and is positioned between the fourth ceratobranchials. An U-shape ligament connects the cupula posteriorly to each of the processes on the ventral surfaces of the third hypobranchials. This semi-circular ligament was originally considered to be characteristic of acanthopterygians (Dietz 1914, as cited by Winterbottom 1974a; Stiassny 1992), but has been identified in several non-acanthopterygians (Springer & Johnson 2004). Additional ligaments connect hypobranchials 2 and 3. The ventral aorta ascends and passes just anterior to the cartilaginous pedicle.

Sphincter oesophagi (SphOes, Figs. 10-11, 13). This muscle is comprised of many autonomous bundles and fibers. Perhaps the most obvious bundles circumscribe the esophagus. In doing so, they may grade with the obliquus posterior. Fibers also parallel the posterior borders of transversus dorsalis III/IV and transversus ventralis V and may grade with either muscle. One sphincter bundle holds the retractor dorsalis against the esophagus acting as a 'belt'. Additional sphincter bundles lie medially and laterally to the retractor dorsalis as the fibers run from the esophagus to the dorsal side of pharyngobranchial 3.

Obliqui ventrales (OV I-III, Fig. 13). Three obliquus ventralis muscles connect the ceratobranchials with their respective hypobranchials across their ventral

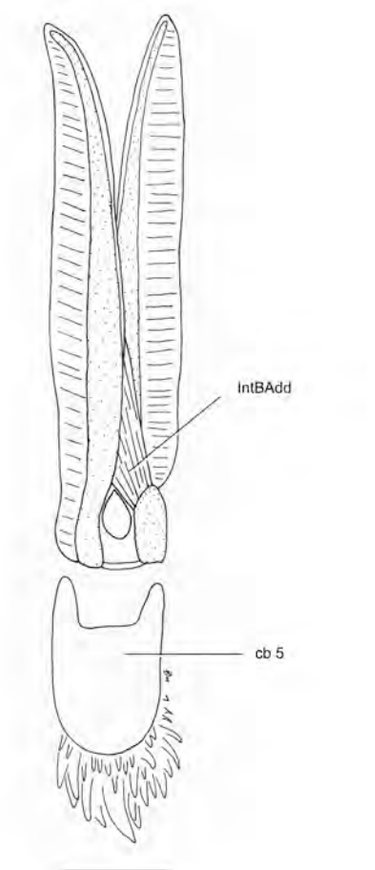

Figure 12. Dorsal view of a gill filament from the transverse section of the left, ceratobranchial 3 of *M. p. punctulatus* (OSUM 102598, 144.7 mm SL). Anterior is to the left. Scale bar = 1 mm. The interbranchiales abductores were not included but would connect either side of the ceratobranchial to the bases of the gill filaments. Abbreviations: IntBAdd – interbranchialis adductor; as in Figure 11.

surfaces. The majority of each muscle lies on the hypobranchials while the ceratobranchials contain strong tendinous attachments. Some fibers of obliquus ventralis III also attach to the U-ligament. By definition, these latter fibers comprise rectus ventralis III, and the resulting bundle is a graded obliquus ventralis III and rectus ventralis III.

Recti ventrales (RV IV, Fig. 13). A single rectus ventralis IV connects the ventral side of ceratobranchial 4 to the U-ligament. Antimeres converge slightly toward the ligament. A fascia extends dorsally along the margins of rectus ventralis IV and the rectus communis forming a longitudinal branchial wall. This fascia extends posteriorly and attaches to ceratobranchial 5 immediately posterior to transversus ventralis IV. *M. treculii* (ROM 1784CS) possesses an extra bundle of rectus ventralis IV originating on the left ceratobranchial 4 and inserting on the U-ligament. *Centrarchus macropterus* (UMMZ 164961) also has an additional rectus bundle originating on ceratobranchial 4, passes ventral to transversus ventralis IV, and inserts tendinously on the posterior side of the cupula at its base.

Transversi ventrales (TV IV-V, Fig. 13). Transversus ventralis IV connects the medial surfaces of ceratobranchials 4 across the midline in the absence of a raphé. The posterior border is ventral to the anterior border of transversus ventralis V. Transversus ventralis V connects the fifth ceratobranchials in a similar manner. The posterior border of transversus ventralis V is continuous with sphincter oesophagi with some fibers appearing to grade with it. Dorsally, the transversi ventrales attach to skin between the ceratobranchials.

Rectus communis (RComm, Fig. 13). Antimeres insert on the lateral surfaces of the urohyal and are graded above its dorsal edge. Antimeres diverge posteriorly and pass medially to ligaments connecting the urohyal and hypobranchials 2 and 3. They insert tendinously on the ventrolateral edges of the fifth ceratobranchials, lat-

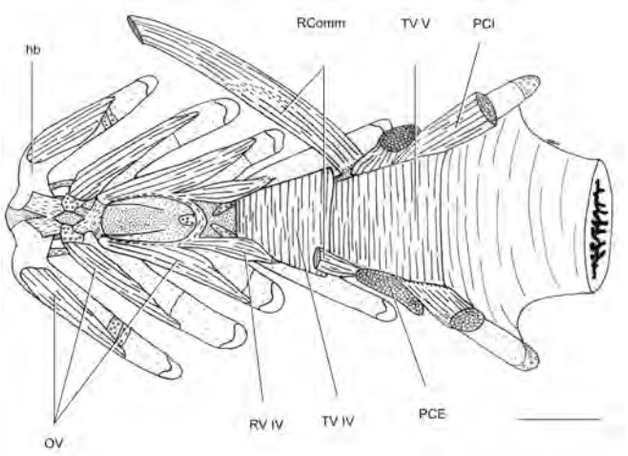

Figure 13. Ventral view of the branchial gill arch musculature of *M. d. dolomieu* (OSUM 102600, 155.2 mm SL). Anterior is to the left. Scale bar = 5 mm. The hyoid arch has been removed and the rectus communis cut away from the urohyal. The right antimere of the rectus communis has been cut near its insertion. Abbreviations: hb – hypobranchial; OV – obliquus ventralis; PCE – pharyngoclavicularis externus; PCI – pharyngoclavicularis internus; RComm – rectus communis; RV – rectus ventralis; TV – transverses ventralis.

eral to the insertions of pharyngoclavicularis externus and internus. The rectus communis may become tendinous as it passes lateral to the ventral aorta.

V. MUSCLES BETWEEN THE PECTORAL GIRDLE AND THE SKULL, HYOID, AND BRANCHIAL ARCHES

Sternohyoideus (StHyo, Figs. 8, 14-15). The sternohyoideus originates on the dorsal surface of the ventral arm of the cleithrum, lateral and anterior to the origin of pharyngoclavicularis externus. Antimeres are heavily graded and contain three myocommata. The bundles pass anteriorly and insert on the lateral sides of the urohyal. Connective tissue from the sternohyoideus extends dorsally and attaches to the ventral processes of hypobranchials 2 and 3. The sternobranchialis, which is derived from the sternohyoideus and attaches to the third hypobranchial, is absent.

Pharyngoclavicularis externus (PCE, Figs. 13-15). This muscle originates on the dorsal surface of the ventral arm of the cleithrum. It passes vertically to insert tendinously on the ventral side of ceratobranchial 5. Length of its insertion is almost that of transversus ventralis V.

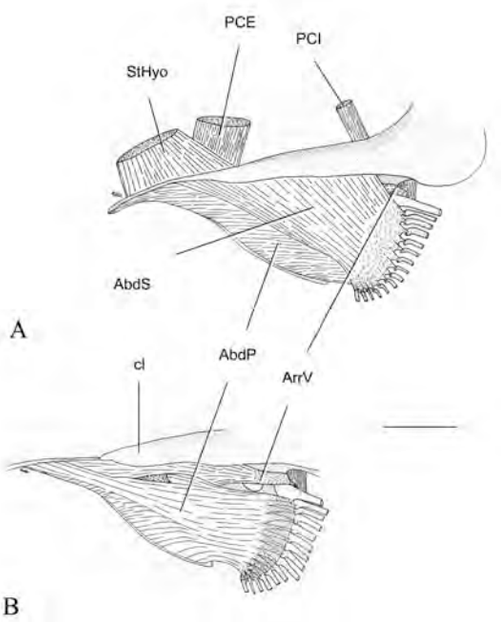

Figure 14. Left, lateral view of the pectoral fin (15 rays) and girdle of *M. treculii* (UMMZ 220247, 137.2 mm SL). Anterior is to the left. Scale bar = 5 mm. A. Superficial abductor muscles and those attaching to the cleithrum from the branchial and hyoid arches. B. Medial abductor muscles. Abbreviations: AbdP – abductor profundus; AbdS – abductor superficialis; ArrV – arrector ventralis; cl – cleithrum; StHyo - sternohyoideus; as in Figure 13.

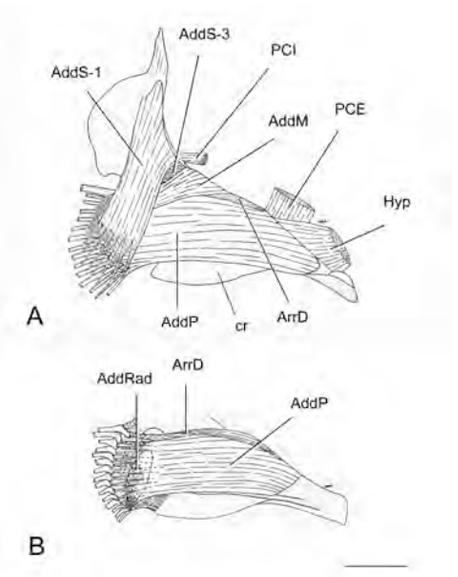

Figure 15. Left, medial view of the pectoral fin (15 rays) and girdle of *M. treculii* (UMMZ 220247, 137.2 mm SL). Anterior is to the right. Scale bar = 5 mm. A. As above. B. After removal of the adductor superficialis bundles. The adductor radialis is outlined by the dashed line. Abbreviations: AddM – adductor medialis; AddP – adductor profundus; AddRad – adductor radialis; AddS – adductor superficialis; ArrD – arrector dorsalis; cr - coracoid; as in Figures 13 - 15.

Pharyngoclavicularis internus (PCI, Figs. 13-15). This muscle originates on the medial surface of the cleithrum near the 'bend' at the juncture of the dorsal and ventral arms. The bundle passes horizontally to insert tendinously on the ventral side of ceratobranchial 5, medial to the pharyngoclavicularis externus. The insertion occupies a small area near the posterior border of transversus ventralis V. *Pomoxis nigromaculatus* (ROM 82440) is unique in that the anterior portions of both antimeres continue anteriorly and insert tendinously on the tips of ceratobranchial 5. In doing so, this anterior extension passes dorsal to transversus ventralis IV.

Protractor pectoralis (PrPect, Fig. 7). This is a well-developed muscle posterior to the muscles serving the dorsal elements of the branchial arches. It originates tendinously on the wing of the pterotic and passes ventrally where it grades into the branchial wall. At the point where muscle fibers disappear, the branchial wall attaches strongly to the cleithrum, dorsal to pharyngoclavicularis internus and ceratobranchial 4.

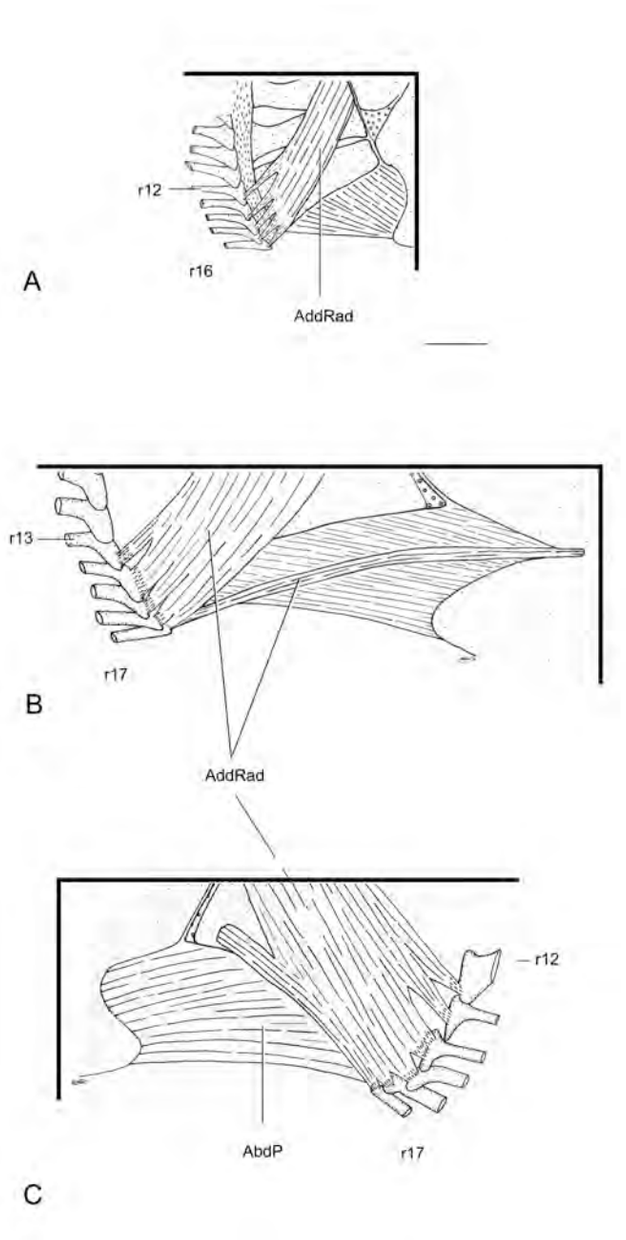

Figure 16. Different patterns of the origin and insertion of the adductor radialis of the pectoral fin. Pectoral rays served have been numbered with the leading ray as ray 1. Scale bar = 1 mm. A. Medial view of the left pectoral fin (16 rays) of *M. notius* (TU 9775, 107.4 mm SL) after removal of the adductor muscles. Anterior is to the right. B. Medial view of the left pectoral fin (17 rays) of *M. notius* (UF 57323, 187.6 mm SL) after removal of the adductor muscles. Anterior is to the right. C. Medial view of the right pectoral fin (17 rays) of *M. notius* (UF 57323, 187.6 mm SL) after removal of the adductor muscles. Anterior is to the left. Abbreviations: r – ray number; as in Figures 14-15.

Levator pectoralis (LPect, Figs. 2, 6, 7). The most obvious fibers of this muscle originate on the pterotic and intercalar and insert on the cleithrum and posttemporal. Perfunctory attention was paid to this muscle so additional attachment sites are not described.

Baudelot's ligament. Although possessing no muscle fibers, this ligament passes from the exoccipital to a vertical ridge on the medial side of the supracleithrum.

VI. MUSCLES OF THE PECTORAL FIN

The pectoral girdle consists of the cleithrum, coracoid, scapula, and four radials with which the rays articulate. An interosseus septum occurs between the coracoid and cleithrum. The number of fin rays varies from 14 to 17 in *Micropterus*, and spines are absent in all species. The first ray is the most robust and referred to as the marginal or leading ray. The interradialis pectoralis is absent in all specimens dissected.

Abductor superficialis (AbdS, Fig. 14). This muscle originates on the posterior side of the lateral flange of the cleithrum. The individual tendons form a continuous aponeurotic sheet and insert on the anterior surfaces of the fin ray bases of all but the marginal or leading ray.

Abductor profundus (AbdP, Figs. 14, 16). This muscle is medial to the abductor superficialis and originates primarily on the lateral surface of the coracoid but also includes the cleithrum near its ventral tip and the interosseus septum between these two bones. The lateral surface of the muscle often has a vertical ridge that coincides with the ventral border of the abductor superficialis. The development of this ridge is variable across specimens. The insertion site is the ventral surface of the posteriorly directed flange at the base of the fin ray. Insertion is tendinous on all rays. The tendon serving the leading ray arises from fibers only partially separated from the main abductor mass. The size of the ray and the tendon serving it decrease at the trailing end of the fin.

Arrector ventralis (ArrV, Fig. 14). The arrector ventralis lies anterior to the abductor profundus and medial to the abductor superficialis. It originates primarily on the cleithrum but also includes the anterodorsal corner of the coracoid and the interosseus septum. Insertion is on the anteromedial surface of the leading ray via a well-developed tendon.

Adductor superficialis (AddS §1-3 and AddM, Fig. 15). Three bundles comprise the adductor superficialis. The distinct middle bundle is given the name of adductor superficialis medialis. Bundle one (§1) is the most medial section and originates on the dorsal arm of the cleithrum. It is vertically orientated and inserts on

the more ventral fin rays. The adductor superficialis medialis (§2 - AddM) is oblique to §1 and originates on the cleithrum along the bend where the dorsal and ventral arms converge. Section 2 serves the middle fin rays. The third section originates on the cleithrum, dorsal corner of the coracoid, and usually the ventral border of the scapula and the interosseus septum. Section 3 is twisted such that tendons from the ventral border of the bundle serve the dorsalmost fin rays. Tendons insert on the anterodistal surfaces of the base of all but the leading fin rays. Tendon length is greatest near ray 8.

Adductor profundus (AddP, Fig. 15). The profundus muscle is lateral and ventral to the adductor superficialis. Origin includes the cleithrum, coracoid, and interosseus septum. Insertion is tendinous on the ventral surface of a posteriorly directed flange of the fin ray. It is noteworthy that tendons serving the ventralmost three rays are greatly reduced in size, and tendons serving the last two fin rays are closely bound to the antepenultimate tendon. Their small size and hidden appearance in combination with neighboring connective tissue create uncertainty in determining the number of ventralmost rays served. In the majority of specimens, all rays except the leading ray are served. Thorsen and Westneat (2005) report variable insertion patterns, such as those noted above, in labroids and five additional percomorph families.

Arrector dorsalis (ArrD, Fig. 15). It originates on the cleithrum, coracoid, and interosseus space between cleithrum and coracoid and inserts on the leading ray. This muscle is graded with the adductor profundus.

Adductor radialis (AddRad, Figs. 15-16. Table 1). This muscle is small and lateral to the adductor profundus. It originates on the medial sides of radials 2-4. Anteriorly fibers may also originate on a fine ridge of the scapula. Insertion is tendinous on the ventralmost fin rays, the number of which is variable both within species and individuals (Table 1). In many instances when the specimen is asymmetrical with respect to the number of fin rays, the fin with the additional ray usually has an additional tendon of the adductor radialis although this pattern is not constant. Given the small size of the tendons, it is possible that some inconsistencies may be the result of observation error, although Thorsen and Westneat (2005) also find interspecific variation of the adductor radialis among labroids and five additional families of coral reef fishes.

Sometimes muscle fibers of the adductor radialis are found that originate separately on the ventromedial face of radial 4 [*M. coosae*, OSUM 105299 (Right side); *M. notius*, UF 57323 (R), UF 58761 (L); *M. p. punctulatus* USNM 251991 (88.0 mm SL) (R); *P. nigromaculatus*, ROM 82440 (L, R)] or the coracoid at its deepest indentation [*M. coosae*, OSUM 105299 (L), ROM 82449 (R); *M. notius*, UF 57323 (L); *M. p. punctulatus*, OSUM 102597 (L); *M. s. salmoides*, ROM 1782CS; *M. treculii*, UMMZ 136849 (L); *L. gibbosus*, ROM 82439 (L, R)]. A single specimen may have multiple conditions.

These fibers comprise a small slip of the adductor radialis that is lateral to the adductor profundus and clearly separable from the more lateral abductor profundus which is exposed in medial view between the coracoid and fourth radial. This slip is separable from the adductor radialis at its origin but then grades to varying degrees with the main adductor mass. A tendon of the slip inserts on the last fin ray and is generally either posteriorly (if from radial 4) or laterally (if from the coracoid) displaced relative to tendons from the adductor radialis although it passes into the main mass prior to insertion in *L. gibbosus* (ROM 82439).

Coracoradialis. Fibers originate from the coracoid near its deepest indentation and attach tendinously to a process on the ventromedial face of radial 4 in *M. treculii* (OSUM 105227, ROM 1784CS). This process occurs distally at approximately one-third the length of radial 4 and is not observed in other dissected centrarchids. The muscle is lateral to the adductor profundus and medial to a translucent connective sheet between radial 4 and the coracoid. These two specimens of *M. treculii* are the largest black bass (> 250 mm SL) dissected and originate from hatchery ponds (G. Garrett, pers. comm.). Fibers in this same orientation are present in *M. d. dolomieu* [OSUM 102599 (L), 173.2 mm SL; ROM 82437 (R), 133.2 mm SL] but attach proximally on the ventromedial surface of the fourth radial in the absence of a process.

VII. MUSCLES OF THE PELVIC FIN

The pelvic fin contains one spine and five rays. The rays are numbered from 1-5 with ray 1 adjacent to the spine and ray 5 being the most medial. Only *M. s. salmoides* (ROM 1780CS) deviated from this pattern with a pelvic fin of I4 (bilaterally).

Abductor superficialis pelvicus (AbdSP, Fig. 17). The abductor superficialis pelvicus originates on the abductor profundus pelvicus, posterior end of the basipterygium, and a mid-ventral septum where it joins its antimere. It grades to varying degrees with the abductor profundus pelvicus, but the two muscles are most easily separable posteriorly. The muscle extends ~50-60% of the pelvic length and inserts via an undifferenti-

Table 1. Variation in the insertion sites of three striated muscles: adductor radialis (pectoral fin), hypochordal longitudinalis and flexor ventralis externus (caudal fin); number of caecae; and nasal rosette in *Micropterus* and centrarchid species. Standard length (mm) follows the catalogue number for specimens from the same lot. "L" and "R" refer to the left and right sides of the specimen respectively. "N/A" indicates damage to the musculature or clearing and staining prior to dissection. Adductor radialis: A dash separates the number of pectoral fin rays from the number of fin rays served. An asterisk following the number of pectoral fin rays indicates that the last fin ray is a rudiment. Hypochordal longitudinalis, flexor ventralis externus: "D" or "V" refers to caudal fin rays dorsal or ventral to the lateral midline respectively; fin rays are numbered sequentially in either direction from the midline. Rosette: Rosette notation describes the number of folds (movable flaps of epithelium) and ridges (immobile flaps) dorsal and ventral of a longitudinal axis. At the posterior end of the longitudinal axis, a single fold is always present and is denoted "/1/". The number of folds is separated from the number of ridges by a colon. Elements dorsal of the longitudinal axis are left of "/1/" while elements ventral of the axis are right of "/1/". For example, "4:2/1/4:1" indicates 12 rosette elements. Four folds and two ridges are present dorsal to the longitudinal axis, followed by a single fold at the posterior end of the axis, and four folds and one ridge ventral to the axis. Ridges always occurred anterior to folds.

Species and Catalogue Number	Adductor Radialis		Hypochordal Longitudinalis		Flexor Ventralis Externus		No. of Caecae	Rosette Formula		No. of Rosette Elements	
	L	R	L	R	L	R		L	R	L	R
M. cataractae											
ROM 82445	16 - 4	16 - 4	D 5-9	D 4-9	V 1-2	V 1-2	10	5:1/1/5:1	4:2/1/4:1	13	12
UMMZ 168752	16 - 4	16 - 3	D 5-9	D 5-9	V 1-2	V 1-2	12	3:0/1/2:0	N/A	6	N/A
M. coosae											
OSUM 105229	16 - 4	16 - 4	D 4-9	D 5-9	V 1-2	V 1-2	10	3:0/1/3:0	2:1/1/2:1	7	7
ROM 82449	15 - 3	15 - 3	D 5-9	D 5-9	V 1-2	V 1-2	10	3:0/1/3:0	3:0/1/3:0	7	7
ROM 82450	15 - 3	15 - 3	D 6-9	D 4-9	V 1-2	V 1-2	9	3:0/1/2:1	3:0/1/3:0	7	7
UF 86268	15 - 4	15 - 4	D 3-8	D 3-8	absent	absent	10	4:0/1/3:0	4:0/1/3:0	8	8
UF 86313	16 - 4	16 - 3	D 5-9	D 5-9	V 1-2	V 1-2	8	4:0/1/3:1	4:0/1/3:1	9	9
UF 89989	N/A - 5	N/A - 4	D 5-9	N/A	V 1	V 1-2	13	N/A	N/A	N/A	N/A
USNM 168075	14* - 3	16 - 4	D 5-9	D 3-9	V 1-3	V 1-2	11	3:1/1/3:1	3:1/1/3:1	9	9
M. d. dolomieu											
ROM 1783CS	16 - 4	16 – 4	D 6-9	D 5-9	V 1-2	V 1-2	16	N/A	N/A	N/A	N/A
ROM 82436	16 - 4	16 – 3	D 4-9	D 4-9	V 1-2	V 1-2	14	6:0/1/5:0	6:0/1/5:0	12	12
ROM 82437	16 - 4	17 – 5	D 6-9	D 5-9	V 1-2	V 1-2	12	4:0/1/4:0	3:1/1/3:1	9	9
OSUM 102599	16 - 4	16 - 4	D 4-9	D 4-9	V 1-2	V 1-2	12	5:0/1/5:0	4:1/1/2:0	11	8
OSUM 102600	16 - 4	16 - 4	D 5-9	D 5-9	V 1-2	V 1-2	14	4:0/1/4:1	4:1/1/3:2	10	11
M. d. velox											
USNM 116802	17 - 4	17 - 4	D 3-9	D 4-9	V 1-2	V 1-2	10	3:0/1/2:1	3:1/1/2:1	7	8
USNM 128680	16 - 4	16 – 4	D 5-9	D 5-9	V 1-2	V 1-2	12	3:1/1/3:0	3:0/1/3:0	8	7
M. notius											
UF 57323	17 - 5	17 - 6	D 5-9	D 5-9	V 1-2	V 1-2	11	2:0/1/2:0	2:0/1/1:1	5	5
UF 58761 (131.8)	17 - 4	17 - 4	D 5-9	D 5-9	V 1-2	V 1-2	12	4:0/1/4:0	5:0/1/4:1	9	11
UF 58761 (145.2)	16 - 5	16 - 5	D 5-9	D 5-9	V 1-2	V 1-2	11	4:1/1/4:0	4:1/1/4:1	10	11
TU 9775 (107.4)	16 - 5	16 - 5	D 5-9	D 6-9	V 1-2	V 1-2	12	1:0/1/1:0	1:0/1/1:0	3	3
TU 9775 (152.3)	16 - 5	16 - 4	D 6-9	D 5-9	V 1-2	V 1-2	12	1:0/1/1:0	N/A	3	N/A

Table 1. Cont.

Species and Catalogue Number	Adductor Radialis		Hypochordal Longitudinalis		Flexor Ventralis Externus		No. of Caecae	Rosette Formula		No. of Rosette Elements	
	L	R	L	R	L	R		L	R	L	R
M. p. punctulatus											
OSUM 102597	15 - 4	15 - 3	D 5-9	D 5-9	V 1-2	see text	11	4:0/1/4:0	4:0/1/3:1	9	9
OSUM 102598	15 - 3	15 - 4	D 3-9	D 3-9	V 1-2	V 1-2	11	5:0/1/4:1	6:0/1/5:0	11	12
USNM 251991 (95.4)	14 - 2	15 - 3	D 5-9	D 5-9	V 1-2	N/A	11	N/A	N/A	N/A	N/A
USNM 251991 (88.0)	15 - 4	14 - 3	D 5-9	D 5-9	V 1-2	V 1-2	10	3:0/1/3:0	3:0/1/3:0	7	7
M. p. henshalli											
UAIC 10587.15	16 - 4	16 - 4	D 5-9	D 5-9	V 1-2	V 1-2	10	6:0/1/5:0	5:0/1/5:0	12	11
UAIC 12652.19	16 - 5	16 – 4	D 6-9	D 5-9	V 1-2	V 1	10	5:1/1/4:1	4:1/1/4:1	12	11
M. s. floridanus											
UMMZ 158634	15 - 4	15 - 4	D 6-9	D 5-8	V 1-2	V 1-2	37	2:1/1/2:1	2:0/1/2:1	7	6
UMMZ 163350	15 - 4	15 - 4	D 6-9	D 5-9	V 1-2	V 1-2	40	3:1/1/4:0	4:0/1/4:0	9	9
M. s. salmoides											
ROM 1780CS	14 - 3	15 - 4	D 6-9	N/A	V 1-2	V 1-2	26	N/A	N/A	N/A	N/A
ROM 1781CS	15 - 4	15 - N/A	D 6-9	N/A	V 1-2	N/A	29	N/A	N/A	N/A	N/A
ROM 1782CS	14 - N/A	14 - 3	D 6-9	D 6-9	V 1-2	N/A	23	N/A	N/A	N/A	N/A
ROM 82435	15 - 4	15 - 4	D 6-9	D 5-9	V 1	V 1	33	4:0/1/4:0	4:0/1/3:0	9	8
ROM 82446 (153.2)	15 - 3	14 - 2	D 6-9	D 6-9	V 1-2	V 1	30	N/A	3:1/1/3:1	N/A	9
ROM 82446 (173.0)	14 - 3	15 - 4	D 6-9	D 6-9	V 1	V 1	31	4:0/1/3:1	N/A	9	N/A
ROM 82446 (214.4)	15 - 3	16 - 4	D 6-9	D 6-9	V 1	V 1-2	24	4:1/1/3:1	3:0/1/4:0	10	8
ROM 82446 (219.4)	14* - 3	14 - 4	D 6-9	D 6-9	N/A	N/A	27	4:1/1/3:1	3:1/1/3:1	10	9
M. treculii											
OSUM 105227	14 - 4	15 – 5	D 4-9	D 5-9	N/A	N/A	N/A	4:0/1/4:0	N/A	9	N/A
ROM 1784CS	15 - 4	15 - 4	D 4-9	D 4-9	N/A	V 1-2	N/A	N/A	5:0/1/5:0	N/A	11
UMMZ 136849	16 – 4	16 – 5	D 3-9	D 3-9	V 1-3	V 1-3	9	N/A	3:0/1/2:1	N/A	7
UMMZ 220247	15 - 3	15 – 4	D 5-9	D 3-9	V 1-2	V 1-2	N/A	3:0/1/3:0	3:0/1/2:1	7	7
A. ariommus											
ROM 82444	14 - 4	15 - 4	D 4-9	D5-9	V 1-2	V 1-3	7	2:1/1/2:1	3:0/1/2:1	7	7
C. macropterus											
UMMZ 164961	13 – 3	13 - 3	D 5-9	D 5-9	V 1	V 1-2	8	4:1/1/4:1	6:0/1/5:0	11	12
L. cyanellus											
ROM 82438	13 – 3	13 - 3	D 5-9	D 5-9	V 1-2	V 1-2	4	3:0/1/2:1	2:2/1/2:1	7	8
L. gibbosus											
ROM 82439	13 – 2	13 - 3	D 5-9	D 5-9	V 1-3	V 1-3	7	2:2/1/3:1	4:0/1/2:1	9	8
P. nigromaculatus											
ROM 82440	14 – 3	14 - 4	D 7-9	D 6-9	V 1	V 1	8	4:1/1/4:0	4:1/1/4:1	10	11

ated tendinous sheet to the spine and all rays on the anterior surface of their medially directed, basal flanges. Hypaxial fibers attach to this muscle via myocommata and complete separation of the two muscles is very difficult.

Abductor profundus pelvicus (AbdPP, Fig. 17). This long muscle originates on the basipterygium and mid-ventral septum and extends ~80% of the pelvic length. The insertion is tendinous on the dorsal surfaces of the five rays but not the spine.

Arrector ventralis pelvicus (ArrVP, Fig. 17). This muscle originates on the ventral side of the pelvis, lateral to the abductor profundus pelvicus, although some fibers may extend medially onto it. The arrector ventral pelvicus extends to the anterior end of the pelvis but not beyond it. Insertion is tendinous on the proximal, ventral surface of the spine.

Adductor superficialis pelvicus (AddSP, Fig. 17). This muscle originates on the dorsal side of the adductor profundus pelvicus and basipterygium near the posterior pelvic process. Antimeres converge at the midline but are not in contact; the muscle extends ~75% of the pelvic length. Tendons insert on the anterior faces of the medially directed flanges of the spine and first four rays. The fifth ray does not possess a medially directed flange and consequently is not served by the adductor superficialis pelvicus.

Adductor profundus pelvicus (AddPP, Fig. 17). This long muscle originates on the basipterygium and extends to the anterior tip of the pelvis but not beyond it. The tendons form a continuous sheet that attaches to the anterior surfaces of the five rays. This attachment site is ventral to that of the adductor superficialis pelvicus.

Arrector dorsalis pelvicus (ArrDP, Fig. 17). The arrector dorsalis pelvicus originates on the lateral side of the basipterygium. Posteriorly the bundle sits in a well-defined bony groove of the basipterygium. Fibers may extend ventrally onto the arrector ventralis pelvicus. It extends anteriorly ~75% of the pelvic length. A large tendon inserts on the proximal, lateral surface of the spine.

Extensor proprius (ExtP, Fig. 17). This small, but well-developed muscle originates on the adductor superficialis and profundus pelvicus with fascia extending laterally to the basipterygium. Insertion is on the dorsal, distal surface of ray 5, where a small tuberosity is present. *Micropterus coosae* (OSUM 105229) and *M. treculii* (ROM 1784CS) each possess one bundle that attaches to rays 4 and 5, while its antimere attaches to ray 5. The extensor proprius inserts on ray 4 bilaterally in *M. s. salmoides* (ROM 1780CS), which has only four fin rays.

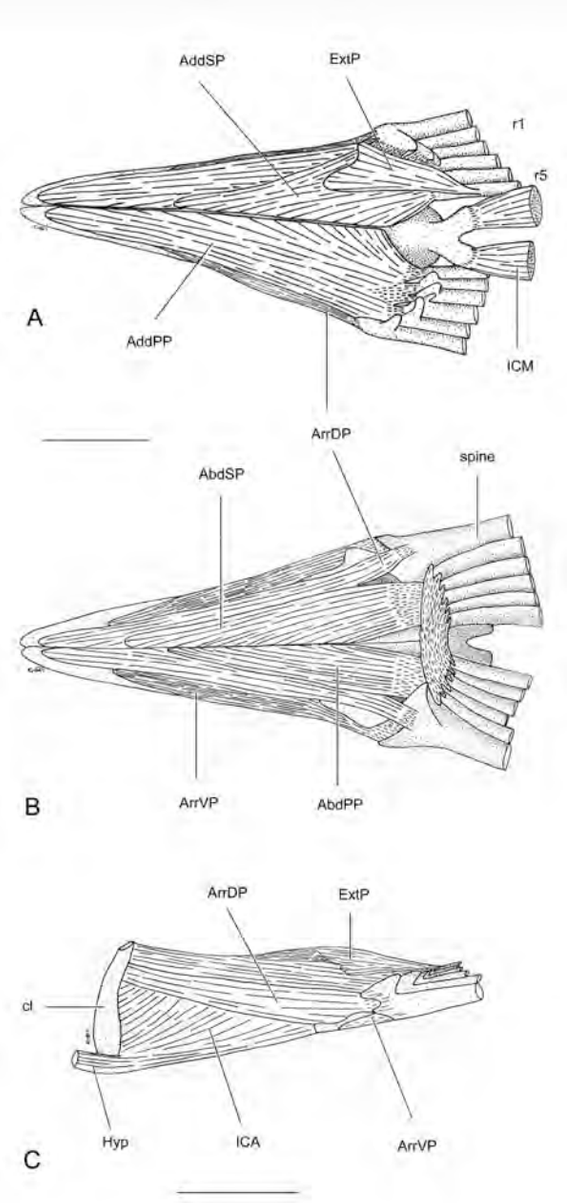

Figure 17. Pelvic fin musculature of *M. s salmoides* (ROM 82446, 153.2 mm SL). Anterior is to the left. Scale bar = 5 mm. A. Dorsal view of the pelvis. The left antimeres of the extensor proprius and adductor superficialis pelvicus have been removed. B. Ventral view of the pelvis. The left abductor superficialis pelvicus antimere has been removed. C. Left, lateral view of the pelvis including the ventral tip of the left cleithrum. Abbreviations: AbdPP – abductor profundus pelvicus; AbdSP – abductor superficialis pelvicus; AddPP – adductor profundus pelvicus; AddSP – adductor superficialis pelvicus; ArrDP – arrector dorsalis pelvicus; ArrVP – arrector ventralis pelvicus; ExtP – extensor proprius; Hyp – hypaxialis; ICA – infracarinalis anterior; ICM – infracarinalis medialis; spine – pelvic spine; as in Figures 14 and 16.

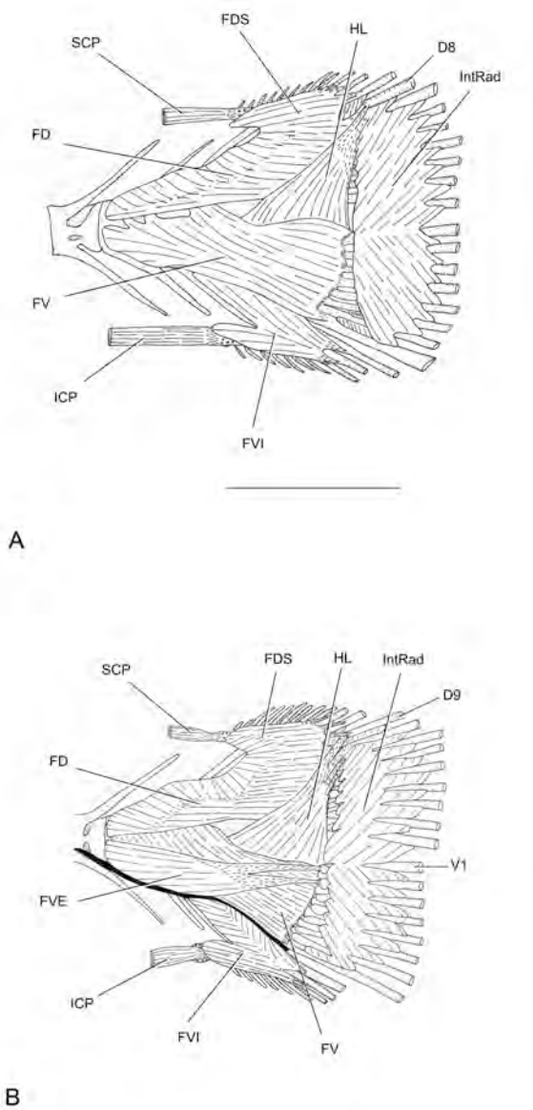

Figure 18. Left, lateral views of the caudal fin musculature. Anterior is to the left. Scale bar = 5 mm. A. *M. coosa*e (UF 86268, 131.8 mm SL) after removal of the epaxialis and hypaxialis. Note that the flexor ventralis externus is missing and the dorsalmost insertion of the hypochordal longitudinalis is to the eighth ray dorsal of the lateral midline. B. *M. p. punctulatus* (OSUM 102598, 144.7 mm SL) after removal of the epaxialis and hypaxialis. The solid black line is a nerve. Abbreviations: D – dorsalmost caudal ray served by the hypochordal longitudinalis; FD – flexor dorsalis; FDS – flexor dorsalis superior; FV – flexor ventralis; FVE – flexor ventralis externus; FVI – flexor ventralis internus; HL – hypochordal longitudinalis; ICP – infracarinalis posterior; IntRad – interradialis; SCP – supracarinalis posterior; V – ventral caudal rays served by flexor ventralis externus.

VIII. MUSCLES OF THE CAUDAL FIN

There are 17 principal caudal rays in black bass; nine dorsal and eight ventral to the midline. The outermost principal caudal rays are segmented and unbranched (Schultze & Arratia 1989). These rays are numbered sequentially beginning at the midline, with those dorsal and ventral to the midline denoted "D" and "V" respectively. Thus, "V6" is the sixth principal caudal ray ventral to the midline. Along the dorsal and ventral margins of the caudal fin are a variable number of procurrent rays which may be segmented but are unbranched (Schultze & Arratia 1989). The caudal fin of *Micropterus* species is typically composed of three epurals, two uroneurals, and five autogenous hypurals. The ural complex (pU1 and caudal centra) is ossified and fused as a single entity. Vertebrae anterior to the ural complex are denoted "pU#" starting with pU2 and sequentially numbered anteriorly. The neural spine of pU2 is short. Cartilaginous distal radials lie distal to the neural and hemal spines of pU3-pU4 or pU4-pU5 and anterior to the procurrent caudal rays. The adductor dorsalis is absent in all species observed.

Interradialis (IntRad, Fig. 18). The interradialis originates and inserts on caudal rays and usually overlaps several fin rays. These bundles span from V8 to D8 or D9. In addition, separate bundles occur between D9-10 and D8-10. At the middle of the fin, fibers originate from a single attachment site on V1 proximally and insert broadly along the ventral side of D1. Medially this arrangement is reversed with fibers originating on D1 and fanning onto V1.

Hypochordal longitudinalis (HL, Fig. 18. Table 1). This muscle is asymmetrical and originates on the ural complex, hypurapophysis, head of the hypural, hypural plates 1-3, and in some specimens on the centrum of pU2. Insertion is tendinous on a variable number of fin rays (Table 1). With two exceptions (*M. coosae*, UF 86268; *M. s. floridanus* UMMZ 158634), the dorsalmost fin element is D9. The tendon serving D9 is the largest. The site of attachment is the anteroventral corner of the ventralmost fin ray, but the site moves distally on more dorsal fin rays. Often the tendon serving the ventralmost ray 'hides' against the posteromedial surface of the preceding tendon thus leading to erroneous observations. Removal of singular and minor variants reveals D5-9 as the generalized condition with *M. s. floridanus* and *M. s. salmoides* characterized by D6-9.

Flexor dorsalis (FD, Fig. 18). The flexor dorsalis originates on the centra and neural spines of pU2-5, ural complex, epurals, uroneurals, hypural plates 4-5 and variably on hypural plate 3. Insertion is tendinous on the

anterior ends of D1-8 with the insertion moving to the lateral surface at D8.

Tendons serving D7 and D8 become 'stringy', meaning that they appear to be comprised of multiple strands and therefore multiple insertion sites. On many specimens, two tendons appear to insert on D8. One tendon inserts medially in an orientation consistent with tendons of the flexor dorsalis, while a more distal and lateral insertional site is consistent with the flexor dorsalis superior. Under this interpretation, both the flexor dorsalis and flexor dorsalis superior insert on D8 in a majority of specimens. At times, a similar orientation is observed on D7.

Flexor dorsalis superior (FDS, Fig. 18). The flexor dorsalis superior originates muscularly on the epurals, distal tip of neural spine pU3, and tendinously on distal radial at the tips of neural spines pU4 or pU5. This distal radial is serves as an attachment site for the supracarinalis posterior, but the two muscles are not continuous as the flexor dorsalis superior is removable largely without affecting the supracarinalis posterior. The flexor dorsalis and flexor dorsalis superior are graded. The most common insertion is on the dorsal, distal surfaces of D8-D12 but may vary to either D8-D11 or D8-D13.

Flexor ventralis (FV, Fig. 18). The flexor ventralis originates on the parhypural, hypurapophysis, ural complex, hypural plate 1, centra pU2-5, and hemal spines pU2-3. The centrum of pU5 and hemal spine of pU4 may variably be included. Insertion is on the anterior faces of V1-8 with the site moving anterodorsally from V1 to V8.

Flexor ventralis inferior (FVI, Fig. 18). This muscle is chevron shaped and separable from the flexor ventralis. Origin of the dorsal arm includes hemal spines pU2-3 while the ventral arm originates on the distal tip of hemal spine pU4 and distal radials between hemal spines pU3-pU4 or pU4-pU5. The infracarinalis posterior also attaches to this distal radial where some fibers may grade with the flexor ventralis inferior. The most common insertion is on the ventrodistal surfaces of V9-11 but may vary to either V9-V10 or V9-V12.

Flexor ventralis externus (FVE, Fig. 18. Table 1). This small slip of a muscle originates on a combination of centra pU3-5 and hemal spines of pU2-3. Posteriorly, fibers disappear into an aponeurosis which yields long and slender tendons that insert on a variable number of caudal fin rays (Table 1). Often a single tendon will extend to a point between two adjacent fin rays thus appearing to insert on both rays. This pattern was interpreted as a single tendon which should serve a single ray, the dorsalmost of the two rays. The flexor ventralis

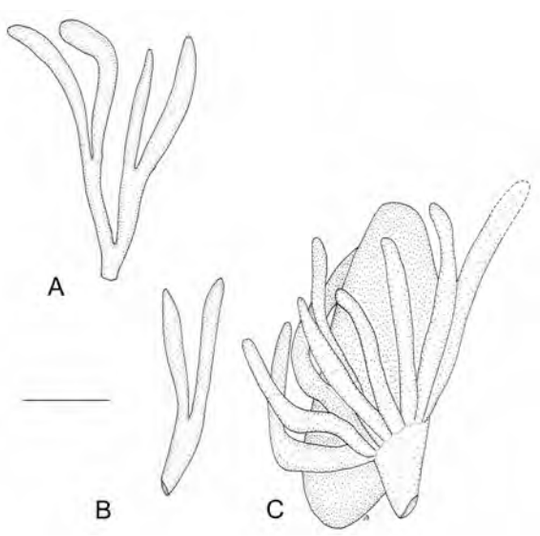

Figure 19. Branching patterns of the pyloric caecae. Scale bar = 5 mm. A. and B. Two observed patterns of branching in *M. s. floridanus* (UMMZ 158634, 128.8 mm SL). C. *M. cataractae* (UMMZ 168752, 102.8 mm SL) has 12 single caecae surrounding the stomach. The intestine has not been included.

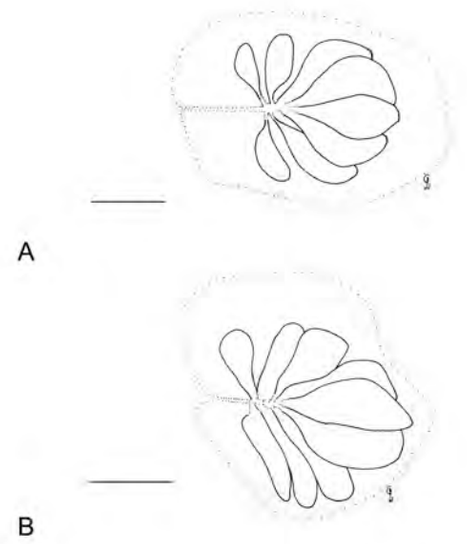

Figure 20. Left, lateral view of the nasal rosette. Dotted line indicates the extent of the nasal capsule. Scale bar = 1 mm. A. *M. coosae* (UF 86268, 131.8 mm SL). Pattern notation is 4:0/1/3:0 as described in Table 1. B. *M. notius* (UF 58761, 131.8 mm SL). Pattern notation is 4:0/1/4:0.

externus grades with the hypaxialis in *M. p. punctulatus* (OSUM 102599) and the flexor ventralis in *M. s. salmoides* (ROM 82446, 219.4 mm). In both instances, their respective insertions remain distinct. *Micropterus coosae* (UF 86268) is unique in lacking a flexor ventralis externus.

IX. NOTES ON OTHER FEATURES OF THE SOFT ANATOMY IN *MICROPTERUS* SPECIES

Pyloric Caecae (Fig. 19). Pyloric caecae are blind sacs that circle the intestine immediately below the stomach. They are assumed to increase retention time of food and therefore serve to facilitate protein digestion and fat or carbohydrate absorption (Barrington 1957). The structure and numbers of caecae are variable among species and absent in other species (e.g. Cyprinidae). The number of caecae and the presence of branched caecae are not independent characters although they are described separately.

Micropterus s. floridanus and *M. s. salmoides* have predominantly branched caecae that occur variably along the length of the caecum. Frequently a caecum has multiple branches resulting in a single base having three, four, and in one instance, seven tips (*M. s. salmoides*, ROM 82446, 153.2 mm). The remaining species of *Micropterus* and other centrarchids have predominantly unbranched caecae. In the majority of these latter exceptions, adjacent branches share part of their walls and thus are caecae not completely separated from each other (*M. coosae* UF 89989, USNM 168075; *M. d. dolomieu* OSUM 102600, ROM 82436; *M. p. punctulatus* OSUM 102597).

M. s. floridanus and *M. s. salmoides* have the most caecae averaging 38.5 and 27.9 respectively. The remaining species of *Micropterus* average 9.0 (*treculii*), 10.0 – 10.8 (*coosae*, *henshalli*, *punctulatus*), 11.0 – 11.6 (*cataractae*, *notius*, *velox*), and 13.6 (*dolomieu*) caecae. The single specimen of each outgroup species has eight (*Pomoxis*, *Centrarchus*), seven (*Ambloplites*, *Lepomis gibbosus*), or four (*Lepomis cyanellus*) caecae (Table 1). If branches are ignored, *M. s. floridanus* and *M. s. salmoides* average 14.0 and 10.0 bases respectively and fall within the range of other *Micropterus* species.

Nasal rosette (Figs. 20, 21. Table 1). The nasal rosette consists of a number of folds in the nasal epithelium arranged above and below the longitudinal axis of the nasal cavity, with a single fold at the posterior end of this axis. This arrangement results in an odd number of folds with an equal number of folds above and below the longitudinal axis. 'Folds' and 'ridges' were differentiated based on their flexibility. A fold is defined as flex-

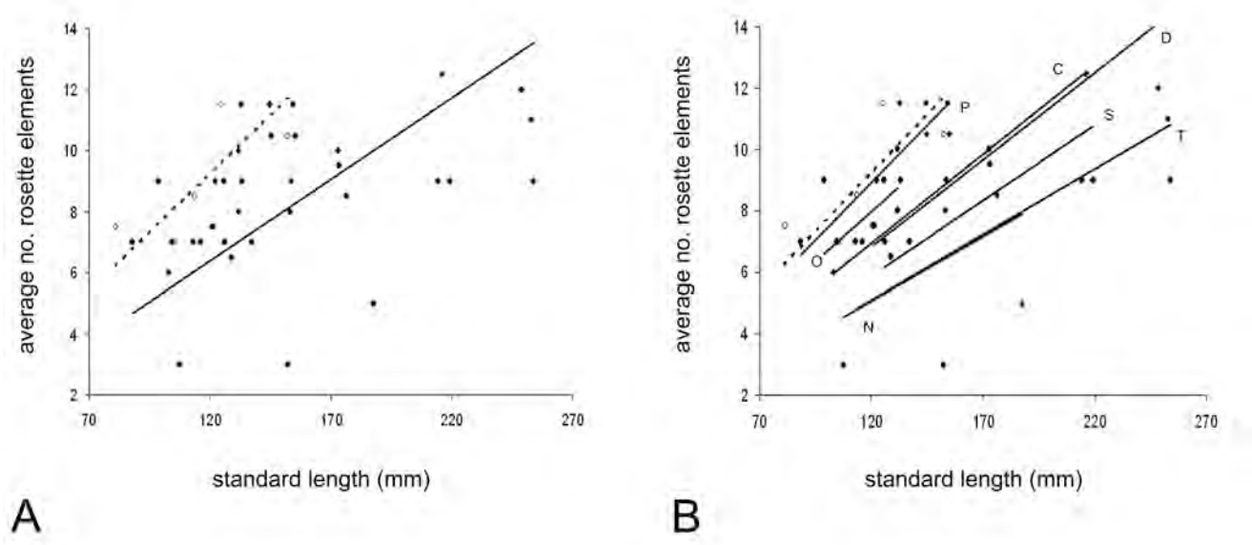

Figure 21. A. Scatterplot of the average number of rosette structures (folds and ridges) per specimen against standard length for *Micropterus* species (filled circles, solid line) and outgroups (open circles, dashed line). B. Scatterplot of the average number of rosette structures per specimen against standard length for each *Micropterus* and outgroup species. Subspecies have not been differentiated. Lines of best fit were forced through the origin. Abbreviations: C – *M. cataractae*; D – *M. dolomieu*; N – *M. notius*; O – *M. coosae*; P – *M. punctulatus*; S – *M. salmoides*; T – *M. treculii*s.

ible piece of tissue that 'flops' when pushed with a probe, whereas a ridge is immobile resembling a speed bump. Folds are always posterior to ridges. The fold is simple, not crenulated, such that a cross-section resembled a keyhole. In the notation below, the number of folds precedes the number of ridges and is separated by a colon. A backslash on either side of "1" represents the single fold along the horizontal axis. The number of folds and ridges ventral of the axis follows in a format consistent with the number of dorsal structures (Table 1). For example, the rosette pattern "4:1/1/3:2" has 11 structures in total. Dorsal to the axis are four folds and a single ridge, followed by a single fold parallel to the longitudinal axis. Three folds and two ridges are ventral to the axis.

Rosette size and the number of elements within the rosette increase with standard length. Variation in standard length explained 47% and 20% of the variation in the number of rosette elements for outgroup and ingroup species respectively (Fig. 21A). Analysis by ingroup species resulted in five clusters of species (Fig. 21B). The positive relationship between standard length and the number of rosette elements is supported by observations that smaller (ridges) and 'missing' elements (denoted by appropriate spaces) are found at the anterior end of the rosette. Posterior elements (folds) are always larger and thus presumably older than more anterior elements (ridges). In instances of asymmetry above and below the longitudinal axis, elements on the dorsal side of the longitudinal axis are either more numerous or more developed than elements below the longitudinal axis.

DISCUSSION

MYOLOGICAL NOTES

Myological descriptions of *Micropterus* are consistent with the conditions of other teleosts (Winterbottom 1974a) and specific observations of the dorsal branchial arch muscles in *M. dolomieu* (Springer & Johnson 2004). A "universal division" (Wu & Shen 2004) of the adductor mandibulae originates from the hyomandibula and palatal arch and passes lateral to ramus mandibularis V (RMV) to insert on the Meckelian fossa and a shared myocommatum with A*ù*. Wu & Shen (2004) identify this section as A2â and synonymize it with A2â of Winterbottom (1974a) and A2-A3 of Gosline (1989). The A3 division described herein is the universal division, and the graded A1–A2 section is the A1-A2á bundle *sensu* Wu and Shen (2004). The presence of an A1-A2á bundle with autonomous divisions of A2â and A*ù* in the absence of A3 appears to be a general characteristic of Perciformes (Wu & Shen 2004).

Divisions of the adductor mandibulae have come under recent scrutiny in an effort to determine the reliability of the course of RMV. One school notes that the path of RMV through divisions of the adductor mandibulae is variable and phylogenetically uninformative (Edgeworth 1935; Winterbottom 1974a; Gill & Mooi 1993). An opposing view suggests that the path of RMV may be phylogenetically informative (Gosline 1989; Diogo & Chardon 2000; Nakae & Sasaki 2004; Wu & Shen 2004), with the primary obstacle to robust interpretations being comparisons among non-homologous divisions of the adductor mandibulae. This latter opinion implies that if the problem of non-homology among divisions of the adductor mandibulae is resolved, the path of the RMV would likely contain a recoverable phylogenetic signal (Gosline 1989). Evolutionary models explaining the origin and pattern of division of the adductor mandibulae were then developed (Gosline 1986, 1989; Diogo & Chardon 2000; Wu & Shen 2004). However, such explanations are based on the *a priori* premise that the course of the RMV is a valid taxonomic character. While it is highly probable that nerves, and their paths, retain a phylogenetic signal, we seek to avoid the circularity of employing the path of RMV to identify divisions of the adductor mandibulae. An ontogenetic analysis of the adductor mandibulae may resolve this dilemma and inform the larger issue of using nerves to identify muscles.

MYOLOGICAL VARIATION

Black bass display all four classes of myological variation: minor, incongruous, singular, and mimicking. Minor variants are slight differences in the size, shape, or position of the muscle arising from a variety of factors including biological (specimen health, age, sex, etc.) and non-biological (storage, preservation) effects. Examples include variable lengths of the pelvic adductors and abductors and the variable origin of the adductor hyomandibulae on the prootic, the pterotic, or both bones due to the fimbricate suture between them. By describing the generalized condition of a species, minor variants are necessarily excluded.

Incongruous variants result in nonfunctional muscles and include cases of absent muscles normally present or shifted insertions, which have negated the original function of the muscle. The sole example of a muscle absent in a specimen was the flexor ventralis externus (caudal fin, *M. coosae*, UF 86268).

Singular variants are atypical and unique to a given specimen. Examples from centrarchids include three bundles of rectus ventralis IV (ventral branchial arches) either all serving the U-shaped ligament (*M. treculii*,

ROM 1784CS) or the U-shaped ligament and cupula (*Centrarchus macropterus*, UMMZ 164961) and the shared origin of the flexor ventralis externus (caudal fin) with either the flexor ventralis (*M. s. salmoides*, ROM 82446, 219.4 mm SL) or the hypaxialis (*M. p. punctulatus*, OSUM 102597). Presumably these muscles retain their original functions despite an altered insertion or origin.

Polymorphic states of the adductor radialis (pectoral fin), hypochordal longitudinalis (caudal fin), and flexor ventralis externus (caudal fin) are a result of mimicking variants which atypically resemble the usual condition of another species. Identifying the cause of this variation is problematic but it could result in part from fluctuating developmental conditions or phenotypic plasticity induced by locomotory differences between individuals. While some variation may be the result of dissection errors, safeguards against observer bias were employed. A random dissection order and independent dissections of the bilateral elements in the same individual suggest that intra-individual, intraspecific, and interspecific variation is considerable in black bass.

A fifth, and rare, trait-category characterized by a high frequency of diverse morphologies is "explosive" variation (Raikow et al. 1990). The breadth of variation in the adductor radialis (pectoral fin) might be considered explosive and likely results from a combination of mimicking and singular variants. In addition, an unexplained compensatory mechanism exists whereby the number of pectoral rays served by the muscle co-varies with the number of fin rays present, even within the same specimen. If meristic variation such as the number of fin rays can influence the number of insertion sites, a similar pattern between muscles and other serial bony elements might be expected. The extensor proprius (pelvic fin) inserts on the medialmost ray, which is usually the fifth ray in black bass; however, it can insert on the fourth ray in the absence of the fifth ray (*M. s. salmoides*, ROM 1780CS).

Finally, specimens possessing one incongruous or singular variant often possessed a second or third variant. Why variants accumulate in some individuals is not clear, but a variety of intrinsic (genetics, life history, body size – Billerbeck et al. 1997, McDowall 2003) and extrinsic (fluctuating environmental conditions – e.g., Gabriel 1944, Hubbs 1959) factors experienced during development are long known to affect the meristics of serial bony elements. For instance, an increase in vertebrae but a decrease in anal fin rays is attributed to colder water temperatures experienced by larval *M. p. punctulatus* at two of nine locations in the Ohio River (Bryan 1969). Observations from the present study suggest that co-variation in the number of fin rays and the number of insertion sites occurs in the adductor radialis (pectoral fin) and the extensor proprius (pelvic fin). For example, bilateral differences in the number of pectoral fin rays occurred in seven specimens, and in six of those the number of rays served by the adductor radialis increased as the number of fin rays increased. If environmental conditions affect meristic variation and myological variation is tied to the meristic counts of fins and vertebrae, for instance, then fluctuating environments may also contribute to myological variation. This line of reasoning is in contrast to Raikow et al. (1990, p. 367), who asserted "that neither sexual difference nor individual developmental instability contributes *substantially* to intraspecific myological variation" in passerine birds (emphasis added). How much variation constitutes "substantial" variation is not clear.

MACROEVOLUTIONARY PATTERNS

Micropterus species share a remarkably uniform external morphology characterized by a fusiform body, large mouth, and posterior extension of the median fins. Myologically they display minor variation of the cheek, jaws, branchial and hyoid complexes and slightly more variation in the pectoral and caudal fin complexes. Additionally, Jayne and Lauder (1994) found *M. salmoides* had the least variation in the linear dimensions of the myoseptal system relative to one species each of *Lepomis*, *Pomoxis*, and *Ambloplites*. Ecologically, black bass are ram feeders of elusive prey such as fishes and crayfishes. Biogeographically, black bass and their sister group *Lepomis* (Near et al. 2005) occupy most of the same drainages, but *Lepomis* is more diverse in the Mississippi basin whereas *Micropterus* is more diverse along the Gulf Coast and southeastern Atlantic drainages where *M. cataractae*, *M. coosae*, *M. notius*, *M. p. henshalli*, and *M. s. floridanus* are restricted (Lee et al. 1980). Geographical outliers include *M. treculii* of the Guadalupe River basin in Texas and *M. d. velox* of the Neosho River and tributaries of the Arkansas River on the western slope of the Ozark Plateau (Koppelman & Garrett 2002). The remaining species of black bass are distributed from the southern USA, northward into the Ohio River basin (*M. p. punctulatus*) and Great Lakes including Ontario and Quebec (*M. d. dolomieu*, *M. s. salmoides*) (Scott & Crossman 1973; Lee et al. 1980; Trautman 1981).

Studies of ecological morphology have concluded that a strong relationship exists between feeding anatomy and diet among fish guilds (e.g., Wainwright & Lauder 1992; Wainwright & Richard 1995), although the absence of a direct one-to-one correlation between mor-

phology and function has been noted (Norton 1995; Wainwright et al. 2005; Collar & Wainwright 2006; Dean et al. 2007). A fuller appreciation of the evolution of the family Centrarchidae requires a consideration of the stasis exhibited by one major lineage, *Micropterus,* in comparison to the ecological and morphological variation exhibited by its sister lineage, *Lepomis,* which likely diverged from each other about 25 mya (Near et al. 2005).

The conservatism in *Micropterus* stands in contrast to the morphological diversity of the 12 species of *Lepomis*, which are primarily suction feeders on a range of sedentary to elusive and soft-bodied to hard-bodied prey (Collar et al. 2005). Comparison of the relationship between diet and morphological diversity in *Micropterus* and *Lepomis* supports the assertion that highly diverse diets across *Lepomis spp.* are correlated to changes in those elements of the skull, jaws, and suspensorium related to food acquisition (Lauder 1983; Wainwright & Lauder 1992; Wainwright & Shaw 1999; Collar et al. 2005). The higher rate of evolution in *Lepomis* (Collar et al. 2005) is driven in part by diet or habitat specialization resulting in differential biomechanical efficiencies and is evidence of natural selection acting in a directional manner (Ehlinger 1990; Cutwa & Turingan 2000 and references therein; Thorsen & Westneat 2005; Wintzer & Motta 2005 and references therein; Higham 2007).

The high degree of myological and overall morphological stasis among *Micropterus* species indicates natural selection has been stabilizing, not directional, and suggests that speciation in this lineage is driven not by ecological specialization but more probably by vicariant events, a conclusion also arrived at by Near et al. (2003). At least in this taxonomic example, speciation events in a static lineage may retain a clearer signal of vicariant geological events when compared to a more speciose lineage whose cladogenesis results from a mixture of ecological, behavioral, and life history specialization as well as vicariance.

The majority of speciation events in *Micropterus* occur during great topographic and climatic change during the Cenozoic of North America (Near et al. 2003, 2005). Warm, tropical temperatures with minimal latitudinal variation in the Eocene gave way to more modern conditions of cooler temperatures (drop of mean annual temperature 8.2 ± 3.1 °C, Zanazzi et al. 2007), and seasonal and latitudinal variation in the Oligocene across central North America (Prothero et al. 2003). The early Miocene (23-17 mya) witnessed large-scale changes in the size of the Antarctic ice sheet (Pekar & DeConto 2006). The cooling phase was marked by Antarctic ice sheet expansion during the middle Miocene (~14 mya, Holbourn et al. 2005) and subsequent sea level fluctuations as the Antarctic ice sheet waxed and waned. The timing of late Miocene-early Pliocene sea fluctuations is consistent with the majority of speciation events in *Micropterus* which are dated to this period (Near et al. 2003, 2005). Fluctuating sea levels may have produced vicariant isolation events at watershed levels. Stabilizing selection resulting in conservative black bass morphology and ecology is reflective of a stable river habitat during the late Miocene and early Pliocene. Other morphologically static perciform groups such as moronids and non-darter percids may also be reliable identifiers of historical geological events that resulted in allopatric speciation during this time.

An alternative hypothesis leading to an increased rate of speciation in *Micropterus*, and consequently other lineages of North American freshwater fishes, is secondary effects of the tremendous uplift of the Colorado Plateau in Western North America. During the Miocene, Colorado Plateau uplift began about 20 mya and formed the Colorado River less than 6 mya (Dorsey et al. 2007). The large western uplift of the Colorado Plateau may have resulted in a much lesser but still significant uplift in eastern North America (i.e., exhumation of the Appalachians during the Miocene-Pliocene), with the effect of entrenching some established eastern river systems (eg., the Susquehenna, New River, Green and Cumberland systems), and isolating other drainages along the Gulf Coast and Atlantic. An explanation of eastern North American uplift in the Mio-Pliocene, although speculative, is consistent with the phylogenies of Catostomidae, Ictaluridae, and Percidae where members of basal lineages (*Carpiodes*, *Ictiobus* in Catostomidae, Harris & Mayden 2001; *Ictalurus* and *Pylodictis* in Ictaluridae, Sullivan et al. 2006; *Perca* in Percidae, Wiley 1992) are lower gradient, large river or more lacustrine than derived lineages which occupy higher gradient habitats. The current habitats occupied by *Micropterus*, moderate-sized rivers of moderate to higher gradient, suggest it would be subject to the selective pressure generated by uplift.

PHYLOGENETIC UTILITY

Within the context of this study, muscle complexes in the caudal and pectoral fins exhibit the greatest variation while complexes of the branchial gill arches, cheeks, and pelvic fin are static. The high frequency of mimicking variants in the caudal and pectoral fins necessitates the use of alternative coding methods to incorporate intraspecifically polymorphic characters into phylogenetic analyses (e.g., Wiens & Servedio 1997; Wiens 1999, 2001). Overall, the paucity of myological characters

suitable for phylogenetic analysis at low taxonomic levels, including *Micropterus*, and their relative rarity compared to osteological characters at these same taxonomic levels is a generally supported tenet (Kesner 1994 and references therein; Borden 1998; Diogo 2004). However, across higher taxonomic levels, these five muscle systems (cheek, branchial gill arches, paired fins, caudal fin) are evolutionarily stable complexes that provide numerous myological characters suitable for comparative and systematic analyses of teleosts and perciforms. Higher taxonomic levels usually circumscribe greater ecological diversity, which may yield greater anatomical diversity.

Rightly or wrongly, static lineages are often considered to be generalized starting points when examining ecological, trophic, or morphological diversity within a larger clade. This perception explains in part why generalized species (i.e., members of static lineages) are often selected as outgroups to polarize character transformation series in phylogenetic analyses. Certainly, the interest and attention of many investigators are drawn to diverse and speciose groups where hypotheses of ecologically-driven divergence mechanisms are possible to test, but static lineages resulting from stabilizing selection give a different but equally valuable perspective into the study of evolutionary mechanisms.

Because static lineages are difficult to resolve phylogenetically at low taxonomic levels using morphology, their most efficient application in systematics may be at unraveling higher-level relationships. Conversely, diverse lineages may have higher resolution at lower taxonomic levels but the use of species with specialized morphologies to serve as outgroups or exemplars of clades in higher-level systematics may introduce unintended biases into analyses. Systematists wishing to incorporate myology, and morphology more generally, into macroevolutionary studies at low taxonomic levels might estimate the relative cost in time and effort of muscle dissections by assessing the ecological diversity of the ingroup. A cost-benefit assessment *a priori* may yield more efficient systematic research, although ultimately it is the distribution of character states that is more relevant than the number of characters (Kesner 1994).

ACKNOWLEDGEMENTS

We thank a number of people for the loans and gifts of material including R. Robins, T. Vigliotti, L. Page, and J. Albert (FLMNH), R. Winterbottom (ROM), B. Kuhajda (UAIC), J. Williams, S. Smith, and S. Jewett (USNM), N. Rios and H. Bart, Jr. (TU), D. Catania (CAS), T. Cavender and M. Kibbey (OSUM), D. Nelson (UMMZ), G. Steinhart and R. Stein (OSU), B. Shaner, P. Landford, and J. Biagi (GADNR), G. Garrett (TXDP&W), and J. Williams (USGS-FL). C. Sheil (JCU) kindly made space and time for use of a camera lucida and critiques of the illustrations, and P. Doerder (CSU) patiently endured his ciliate lab smelling of preserved fish. R. Krebs (CSU), D. Franz (FLMNH), and one anonymous reviewer provided valuable critiques of the manuscript. In particular, we thank E. Hilton (FMNH) for a careful review of the manuscript and his many valuable suggestions. The Department of Biological, Geological, and Environmental Sciences (CSU) provided support to WCB.

LITERATURE CITED

Avise, J. C., D. O. Straney, & M. H. Smith. 1977. Biochemical genetics of sunfish IV. Relationships of centrarchid genera. Copeia, 1977:250-258.

Bailey, R. M. 1938. A systematic revision of the centrarchid fishes, with a discussion of their distribution, variations, and probable interrelationships. Ph. D. dissertation. University of Michigan, Ann Arbor. 256 p.

Bailey, R. M., & C. L. Hubbs. 1949. The black basses (*Micropterus*) of Florida, with description of a new species. Occasional Papers, Museum of Zoology, University of Michigan, 516:1-40 + 2 plates.

Barrington, E. J. W. 1957. The alimentary canal and digestion. Pp. 109-161 *in* M. E. Brown, ed. The Physiology of Fishes. Vol. 1 Metabolism. New York: Academic Press, 447 p.

Billerbeck, J. M., G. Orti, & D. O. Conover. 1997. Latitudinal variation in vertebral number has a genetic basis in the Atlantic silverside, *Menidia menidia*. Canadian Journal of Fisheries and Aquatic Sciences, 54:1796-1801.

Blair, Jr., C. B., & W. N. Brown. 1961. The osteology of the red eye bass, *Micropterus coosae* (Hubbs and Bailey). Journal of Morphology, 109:19-36.

Bock, W. J., & C. R. Shear. 1972. A staining method for gross dissection of vertebrate muscles. Anatomische Anzeiger, 130(1):222-227.

Borden, W. C. 1998. Comparative myology of the unicornfishes, *Naso* (Acanthuridae, Percomorpha), with implications for phylogenetic analysis. Journal of Morphology, 239(2):191-224.

Borden, W. C. 1999. Phylogeny of the unicornfishes (*Naso*, Acanthuridae) based on soft anatomy. Copeia, 1999(1):104-119.

Branson, B. A., & G. A. Moore. 1962. The lateralis components of the acoustico-lateralis system in the sunfish family Centrarchidae. Copeia, 1962(1):1-108.

Bryan, C. F. 1969. Variation in selected meristic characters of some basses, *Micropterus*. Copeia,

1969:370-373.

Collar, D. C., T. J. Near, & P. C. Wainwright. 2005. Comparative analysis of morphological diversity: does disparity accumulate at the same rate in two lineages of centrarchid fishes? Evolution, 59(8):1783-1794.

Collar, D. C., & P. C. Wainwright. 2006. Discordance between morphological and mechanical diversity in the feeding mechanism of centrarchid fishes. Evolution, 60(12):2575-2584.

Cutwa, M. M., & R. G. Turingan. 2000. Intralocality variation in feeding biomechanics and prey use in *Archosargus probatocephalus* (Teleostei, Sparidae), with implications for the ecomorphology of fishes. Environmental Biology of Fishes, 59:191-198.

Dean, M. N, J. J. Bizzarro, & A. P. Summers. 2007. The evolution of cranial design, diet, and feeding mechanisms in batoid fishes. Integrative and Comparative Biology, 47(1):70-81.

Dietz, P.A. 1914. Beiträge zur Kenntnis der Kiefer-und Kiemenbogenmuskulatur der Teleostier. I. Die Kieferund Kiemenbogenmuskeln der Acanthopterygii. Mitteilungen Statzione zoological Neapel. 22(4)99-162.

Diogo, R. 2004. Muscles versus bones: catfishes as a case study for a discussion on the relative contribution of myological and osteological features in phylogenetic reconstructions. Animal Biology, 54(4):373-391.

Diogo, R. 2005**.** Morphological Evolution, Aptations, Homoplasies, Constraints and Evolutionary Trends: Catfishes as a Case Study on General Phylogeny and Macroevolution**.** Science Publishers Inc., Enfield, NH, 491 p.

Diogo, R., & V. Abdala. 2007. Compartive anatomy, homologies and evolution of the pectoral muscles of bony fish and tetrapods: a new insight. Journal of Morphology, 268:504-517.

Diogo, R., & M. Chardon. 2000. Homologies among different adductor mandibulae sections of teleostean fishes, with special regard to catfishes (Teleostei: Siluriformes). Journal of Morphology, 243:193-208.

Dorsey, R. J., A. Fluette, K. McDougall, B. A. Housen, S. U. Janecke, G. J. Axen, & C. R. Shirvell. 2007. Chronology of Miocene-Pliocene deposits at Split Mountain Gorge, Southern California: a record of regional tectonics and Colorado River evolution. Geology, 35(1):57-60.

Edgeworth, F. H. 1935. The Cranial Muscles of Vertebrates. Cambridge University Press: Cambridge, 493 p.

Ehlinger, T. J. 1990. Habitat choice and phenotype-limited feeding efficiency in bluegill: individual differences and trophic polymorphism. Ecology, 71(3):886-896.

Freihofer, W. C. 1963. Patterns of the ramus lateralis accessories and their systematic significance in teleostean fishes. Stanford Ichthyological Bulletin, 8(2):81-189.

Gabriel, M. L. 1944. Factors affecting the number and form of vertebrae in *Fundulus heteroclitus*. Journal of Experimental Zoology, 95(1):105-143.

Gill, A. C., & R. D. Mooi. 1993. Monophyly of the Grammatidae and of the Notograptidae, with evidence for their phylogenetic positions among Perciformes. Bulletin of Marine Science, 52:327-350.

Gosline, W. A. 1986. Jaw muscle configuration in some higher teleostean fishes. Copeia, 1986(3):705-713.

Gosline, W. A. 1989. Two patterns of differentiation in the jaw musculature of teleostean fishes. Journal of Zoology, London, 218:649-661.

Greenwood, P. H. 1995. Preliminary studies on a mandibulohyoid 'ligament' and other intrabuccal connective tissue linkages in cirrhitid, latrid and cheilodactylid fishes (Perciformes: Cirrhitoidei). Bulletin of the Natural History Museum, London (Zoology), 61(2):91-107.

Greenwood, P. H., & G. V. Lauder. 1981. The protractor pectoralis muscle and the classification of teleost fishes. Bulletin of the Natural History Museum, London (Zoology), 41(4):213-234.

Harris, P. M., & R. L. Mayden. 2001. Phylogenetic relationships of major clades of Catostomidae (Teleostei: Cypriniformes) as inferred from mitochondrial SSU and LSU rDNA sequences. Molecular Phylogenetics and Evolution, 20(2):225-237.

Higham, T. E. 2007. Feeding, fins and braking maneuvers: locomotion during prey capture in centrarchid fishes. The Journal of Experimental Biology, 210:107-117.

Holbourn, A., W. Kuhnt, M. Schulz, & H. Erlenkeuser. 2005. Impacts of orbital forcing and atmospheric carbon dioxide on Miocene ice-sheet expansion. Nature, 438(7067):483-487.

Hubbs, C. 1959. High incidence of vertebral deformities in two natural populations of fishes inhabiting warm springs. Ecology, 40(1):154-155.

Hubbs, C. L., & R. M. Bailey. 1940. A revision of the black basses (*Micropterus* and *Huro*) with descriptions of four new forms. Miscellaneous Publications, Museum of Zoology, University of Michigan, No. 48, 51 p. plus VI plates, 2 Maps.

Iwami, T. 2004. Comparative morphology of the adductor mandibulae musculature of notothenioid fishes (Pisces, Perciformes). Antarctic Science, 16(1):17-21.

Jayne, B. C., & G. V. Lauder. 1994. Comparative morphology of the myomeres and axial skeleton in four genera of centrarchid fishes. Journal of Morphology, 220:185-205.

Johnson, R. L., J. B. Magee, & T. A. Hodge. 2001. Phylogenetics of freshwater black basses (Centrarchidae: Micropterus) inferred from restriction endonuclease analysis of mitochondrial DNA. Biochemical Genetics, 39(11/12):395-406.

Kassler, T. W., J. B. Koppelman, T. J. Near, C. B. Dillman, J. M. Levengood, D. L. Swofford, J. L. VanOrman, J. E. Claussen, & D. P. Philipp. 2002. Molecular and morphological analyses of the black basses: implications for taxonomy and conservation. Pp. 291-322 *in* D. P. Philipp & M. S. Ridgway, eds. Black Bass: Ecology, Conservation, and Management. AFS Symposium 31. American Fisheries Society, Bethesda, MD, 724 p.

Kesner, M. H. 1994. The impact of morphological variants on a cladistic hypothesis with an example from a myological data set. Systematic Biology, 43(1):41-57.

Koppelman, J. B., & G. P. Garrett. 2002. Distribution, biology, and conservation of the rare black bass species. Pp. 333-341 *in* D. P. Philipp & M. S. Ridgway, eds. Black Bass: Ecology, Conservation, and Management. AFS Symposium 31. American Fisheries Society, Bethesda, MD, 724 p.

Lauder, G. V. 1982. Structure and function in the tail of the pumpkinseed sunfish (*Lepomis gibbosus*). Journal of Zoology, London, 197:483-495.

Lauder, G. V. 1983. Functional and morphological bases of trophic specialization in sunfishes (Teleostei, Centrarchidae). Journal of Morphology, 178:1-21.

Lee, D. S., C. R. Gilbert, C. H. Hocutt, R. E. Jenkins, D. E. McAllister, & J. R. Stauffer, Jr. eds. 1980. Atlas of North American Freshwater Fishes. North Carolina State Museum of Natural History, Raleigh, NC, 854 p.

Leviton, A. E., R. H. Gibbs Jr., E. Heal, & C. E. Dawson. 1985. Standards in herpetology and ichthyology: Part I. Standard symbolic codes for institutional resource collections in herpetology and ichthyology. Copeia, 1985:802-832.

Mabee, P. M. 1988. Supraneural and predorsal bones in fishes: development and homologies. Copeia, 1988:827-838.

Mabee, P. M. 1993. Phylogenetic interpretation of ontogenetic change: sorting out the actual and artefactual in an empirical case study of centrarchid fishes. Zoological Journal of the Linnean Society, 107:175-291.

Mabee, P. M. 1995. Evolution of pigment pattern development in centrarchid fishes. Copeia, 1995(3):586-607.

McDowall, R.M. 2003. Variation in vertebral number in galaxiid fishes (Teleostei: Galaxiidae): A legacy of life history, latitude and length. Environmental Biology of Fishes, 66: 361–381.

Mooi, R. D., & A. C. Gill. 1995. Association of epaxial musculature with dorsal-fin pterygiophores in acanthomorph fishes, and its phylogenetic significance. Bulletin of the Natural History Museum, London (Zoology), 61:121-137.

Nakae, M., & K. Sasaki. 2004. Homologies of the adductor mandibulae muscles in Tetraodontiformes as indicated by nerve branching patterns. Ichthyological Research, 51:327-336.

Near, T. J., T. W. Kassler, J. B. Koppelman, C. B. Dillman, & D. P. Philipp. 2003. Speciation in North American black basses, *Micropterus*, (Actinopterygii: Centrarchidae). Evolution, 57(7):1610-1621.

Near, T. J., D. I. Bolnick, & P. C. Wainwright. 2005. Fossil calibrations and molecular divergence time estimates in centrarchid fishes (Teleostei: Centrarchidae). Evolution, 59(8):1768-1782.

Nelson, J. S., 2006. Fishes of the World. 4th edition. John Wiley & Sons, Inc., Hoboken, NJ, 601 p.

Nelson, J. S., E. J. Crossman, H. Espinosa-Pérez, L. T. Findley, C. R. Gilbert, R. N. Lea, & J. D. Williams. 2004. Common and Scientific Names of Fishes of the United States, Canada, and Mexico. AFS Special Publication 29. American Fisheries Society, Bethesda, MD, 386 p.

Norton, S. F. 1995. A functional approach to ecomorphological patterns of feeding in cottid fishes. Environmental Biology of Fishes, 44:61-78.

Norton, S. F., & E. L. Brainerd. 1993. Convergence in the feeding mechanics of ecomorphologically similar species in the Centrarchidae and Cichlidae. Journal of Experimental Biology, 176:11-29.

Pasztor, V. M., & H. Kleerekoper. 1962. The role of the gill filament musculature in teleosts. Canadian Journal of Zoology, 40:785-802.

Pekar, S. F., & R. M. DeConto. 2006. High-resolution estimates for the early Miocene: evidence for a dynamic ice sheet in Antarctica. Palaeogeography, Palaeoclimatology, Palaeoecology, 231(1-2):101-109.

Philipp, D. P., & M. S. Ridgway, eds. 2002. Black Bass: Ecology, Conservation, and Management. AFS Symposium 31. American Fisheries Society, Bethesda, MD, 724 p.

Potthoff, T. 1984. Clearing and staining techniques. Pp. 35-37 *in* G. Moser, W. J. Richards, D. M. Cohen, M. P. Fahay, A. W. Kendall & S. L. Richardson, eds. Ontogeny and Systematics of Fishes. ASIH Special

Publication, no. 1. American Society of Ichthyologists and Herpetologists, Gainesville, FL, 760 p.

Prothero, D. R., L. C. Ivany, & E. A. Nesbitt. 2003. From Greenhouse to Icehouse: The Marine Eocene-Oligocene Transition. Columbia University Press, New York, 541 p.

Raikow, R. J., A. H. Bledsoe, B. A. Meyers, & C. J. Welsh. 1990. Individual variation in avian muscles and its significance for the reconstruction of phylogeny. Systematic Zoology, 39:362-370.

Ramsey, J. S. 1975. Taxonomic history and systematic relationships among species of *Micropterus*. Pp. 67-75 *in* R. H. Stroud & H. Clepper, eds. Black Bass Biology and Management. Sport Fishing Institute, Washington, D.C., 534 p.

Roe, K. J., P. M. Harris, & R. L. Mayden. 2002. Phylogenetic relationships of the genera of North American sunfishes and basses (Percoidei: Centrarchidae) as evidenced by the mitochondrial cytochrome b gene. Copeia, 2002:897-905.

Schultze, H.-P., & G. Arratia. 1989. The composition of the caudal skeleton of teleosts (Actinopterygii: Osteichthyes). Zoological Journal of the Linnean Society, 97:189-231.

Scott, W. B., & E. J. Crossman. 1973. Freshwater Fishes of Canada. Fisheries Research Board of Canada, Bulletin 184. Ottawa, ON, 966 p.

Shufeldt, R.W. 1900. The skeleton of the black bass. Extracted from the U. S. Fish Commission Bulletin for 1899:311-320, and plate 44.

Springer, V. G., & G. D. Johnson. 2004. Study of the dorsal gill-arch musculature of teleostome fishes, with special reference to the Actinopterygii. Bulletin of the Biological Society of Washington, 11:1-260. 2 Volumes.

Stiassny, M. L. J. 1992. Atavisms, phylogenetic character reversals, and the origin of evolutionary novelties. Netherlands Journal of Zoology, 42(2-3):260-276.

Sullivan, J. P., J. G. Lundberg, & M. Hardman. 2006. A phylogenetic analysis of the major groups of catfishes (Teleostei: Siluriformes) using *rag1* and *rag2* nuclear gene sequences. Molecular Phylogenetics and Evolution, 41:636-662.

Taylor, W. R., & G. C. Van Dyke. 1985. Revised procedures for staining and clearing small fishes and other vertebrates for bone and cartilage study. Cybium, 9(2):107-119.

Thorsen, D. H., & M. W. Westneat. 2005. Diversity of pectoral fin structure and function in fishes with labriform propulsion. Journal of Morphology, 263:133-150.

Trautman, M. B. 1981. The Fishes of Ohio. Revised edition. Ohio State University Press, Columbus, OH, 782 p.

Wainwright, P. C., M. E. Alfaro, D. I. Bolnick, & C. D. Hulsey. 2005. Many-to-one mapping of form to function: a general principle in organismal design? Integrative and Comparative Biology, 45:256-262.

Wainwright, P. C., & G. V. Lauder. 1992. The evolution of feeding biology in sunfishes (Centrarchidae). Pp. 472-491 *in* R. L. Mayden, ed. Systematics, Historical Ecology, and North American Freshwater Fishes. Standford University Press, Stanford, CA, 969 p.

Wainwright, P. C., & B. A. Richard. 1995. Predicting patterns of prey use from morphology of fishes. Environmental Biology of Fishes, 44:97-113.

Wainwright, P. C., & S. S. Shaw. 1999. Morphological basis of kinematic diversity in feeding sunfishes. The Journal of Experimental Biology, 202:3101-3110.

Wiens, J. J. 1999. Polymorphism in systematics and comparative biology. Annual Review of Ecology and Systematics, 30:327-362.

Wiens, J. J. 2001. Character analysis in morphological phylogenetics: problems and solutions. Systematic Biology, 50(5):689-699.

Wiens, J. J., & M. R. Servedio. 1997. Accuracy of phylogenetic analysis including and excluding polymorphic characters. Systematic Biology, 46(2):332-345.

Wiley, E. O. 1992. Phylogenetic relationships of the Percidae (Teleostei, Perciformes): a preliminary hypothesis. Pp. 247-267 *in* R. L. Mayden, ed. Systematics, Historical Ecology, and North American Freshwater Fishes. Standford University Press, Stanford, CA, 969 p.

Winterbottom, R. 1974a. A descriptive synonymy of the striated muscles of the Teleostei. Proceedings of the Academy of Natural Sciences of Philadelphia, 125(12):225-317.

Winterbottom, R. 1974b. The familial phylogeny of the Tetraodontiformes (Acanthopterygii: Pisces) as evidenced by their comparative myology. Smithsonian Contributions to Zoology, 155:1-201.

Winterbottom, R. 1993. Myological evidence for the phylogeny of recent genera of surgeonfishes (Percomorpha, Acanthuridae), with comments on the Acanthuroidei. Copeia, 1993(1):21-39.

Wintzer, A. P., & P. J. Motta. 2005. Diet-induced phenotypic plasticity in the skull morphology of hatchery-reared Florida largemouth bass, *Micropterus salmoides floridanus*. Biology of Freshwater Fish, 14:311-318.

Wu, K-Y., & S-C. Shen. 2004. Review of the teleostean adductor mandibulae and its significance to the systematic positions of the Polymixiiformes,

Lampridiformes, and Triacanthoidei. Zoological Studies, 43(4):712-736.

Yabe, M. 1985. Comparative osteology and myology of the superfamily Cottoidea (Pisces: Scorpaeniformes), and it phylogenetic classification. Memoirs of the Faculty of Fisheries, Hokkaido University, 32:1-130.

Zanazzi, A., M. J. Kohn, B. J. MacFadden, & D. O. Terry, Jr. 2007. Large temperature drop across the Eocene-Oligocene transition in central North America. Nature, 445(7128):639-642.